Magnetic fields and polarization in AGN jets.

John Wardle (Brandeis University)

OUTLINE OF REVIEW

1) Fractional polarization
2) EVPA-jet alignment
3) Models for misaligned EVPAs
4) Radio-optical EVPA alignment
5) Optical polarization
6) Rotation measures
7) Rotation measure gradients: a) observations
   b) interpretation
8) Circular polarization
9) The Event Horizon Telescope

[Project Description]

[Team Members]

[The Sample]

[Data Archive]

[Observational Status]

[Movies]

[RM Maps]

[Publications]

[Outreach]

Useful Links:

[Blazar Monitoring List]

TEVCAT

Bordeaux VLBI Database

BZCAT

[VIPS Survey]

[VLBA 2 cm Survey]

[VSOP Pre-Launch Survey]

[Radio Reference

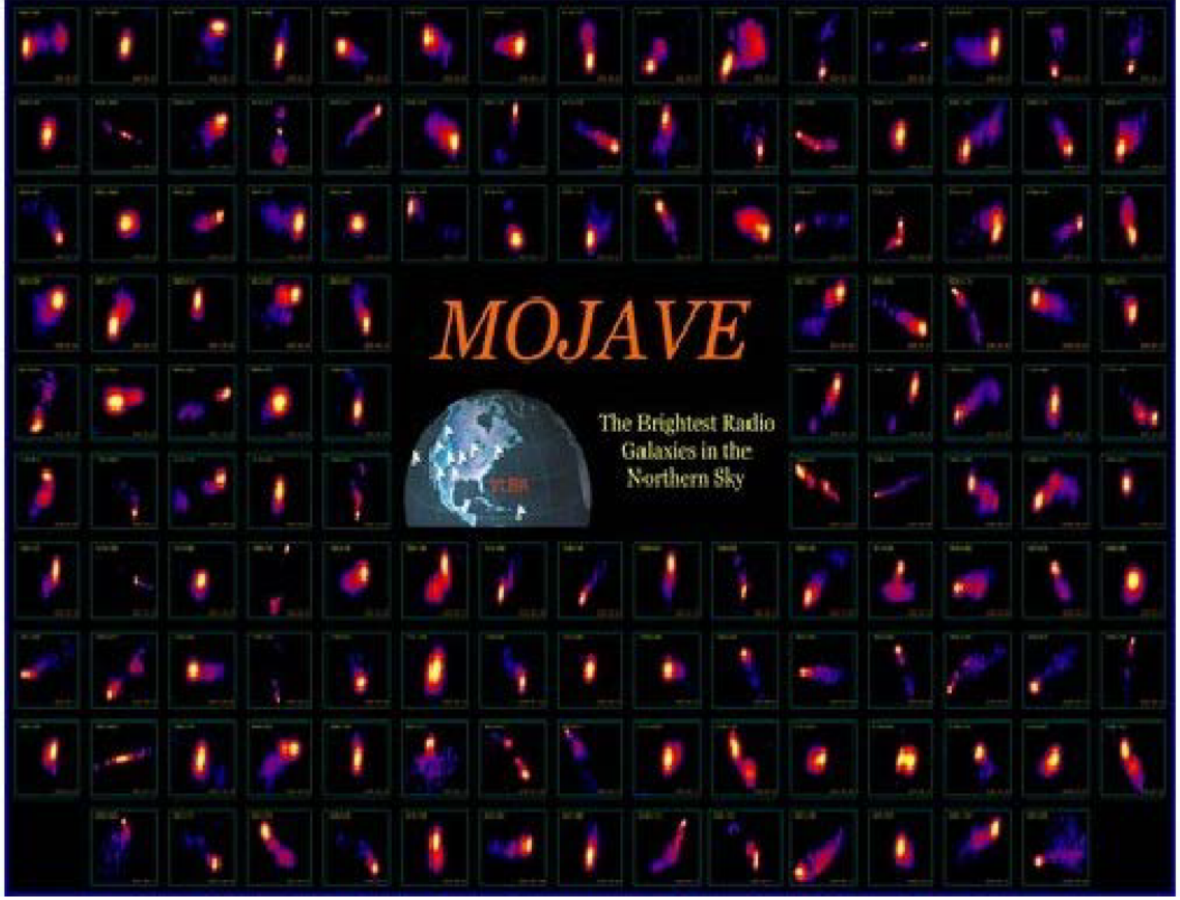

MOJAVE (**M**onitoring **O**f **J**ets in **A**ctive galactic nuclei with **V**LBA **E**xperiments) is a long-term program to monitor radio brightness and polarization variations in jets associated with active galaxies visible in the northern sky. Approximately 2/3 of these were observed from 1994-2002 as part of the [VLBA 2 cm Survey]. These jets are powered by the accretion of material onto billion-solar-mass black holes located in the nuclei of active galaxies. Their rapid brightness variations and [apparent superluminal motions] indicate that they contain highly energetic plasma moving nearly directly at us at speeds approaching that of light. Our observations are made with the world's highest resolution telescope: the [Very Long Baseline Array (VLBA)] at a wavelength of 2 cm, which enables us to make full polarization images with an angular resolution better than 1 milliarcsecond (the apparent separation of your car's headlights parked on the Moon, as seen from Earth). We are using these data to better understand the complex evolution and magnetic field structures of these jets on light-year scales, close to where they originate in the active nucleus, and how this activity is correlated with gamma-ray emission

Linear and Circular Polarization VLBI Observations are Difficult. Understanding Your Errors Is CRUCIAL.

Discussions and simulations of linear polarization, rotation measure and circular polarization imaging and measurement errors in VLBI are essential reading. They include:

Mahud et al. 2013 (Appendix)
Hovatta et al. 2012 (Appendix)
Taylor and Zavala 2010
Homan and Lister 2006
Roberts, Wardle and Brown 1994 (Appendix)

et al.

1) Fractional polarization

Data from MOJAVE at 15 GHz
Lister & Homan 2005

Cores

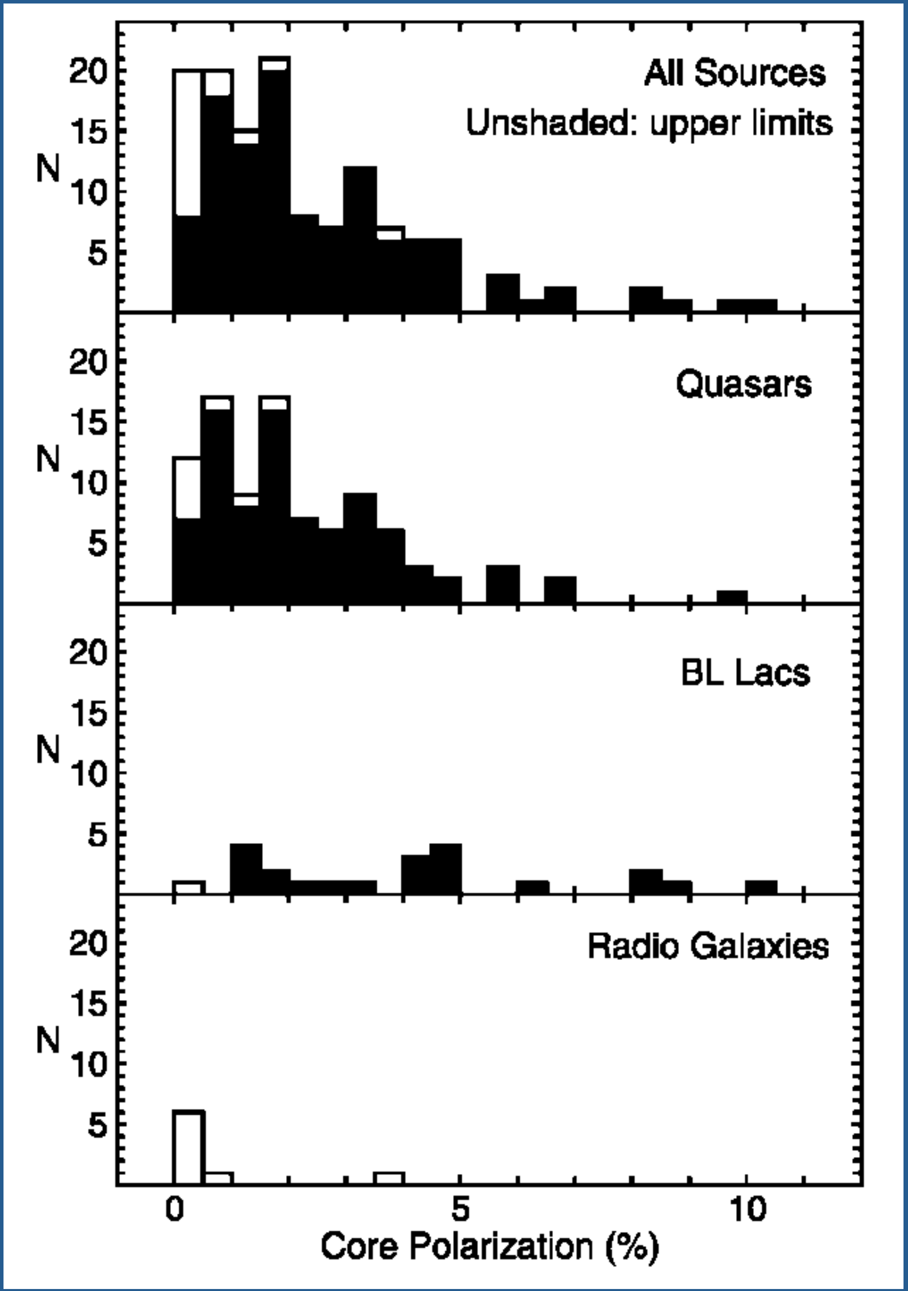

Jet components

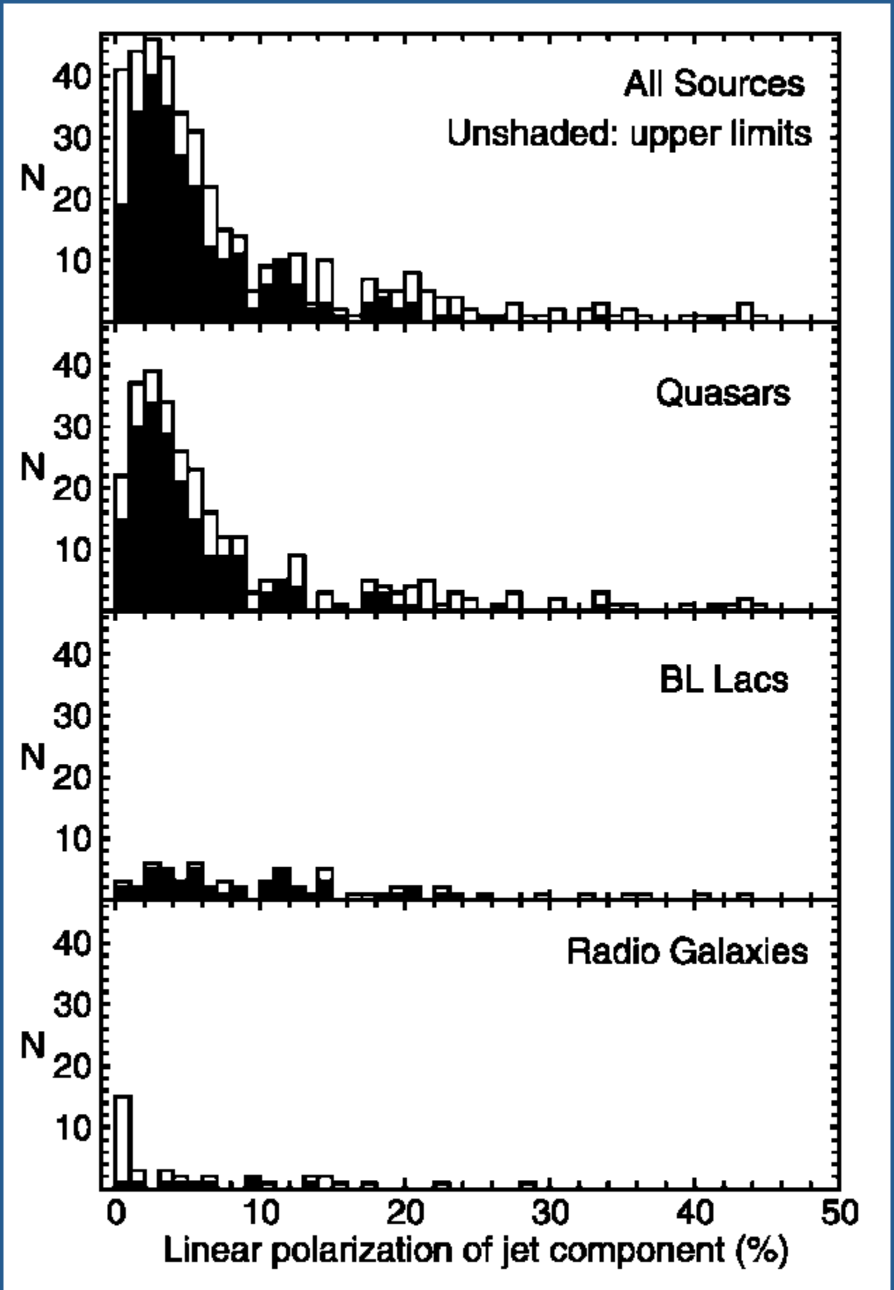

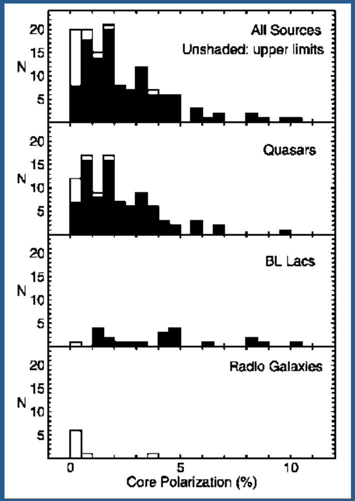
All Sources
Unshaded: upper limits
Quasars
BL Lacs
Radio Galaxies
N
Core Polarization (%)

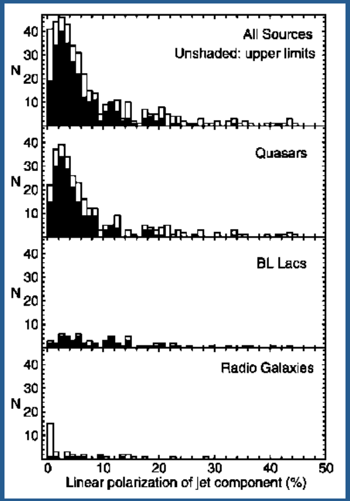
All Sources
Unshaded: upper limits
Quasars
BL Lacs
Radio Galaxies
N
Linear polarization of jet component (%)

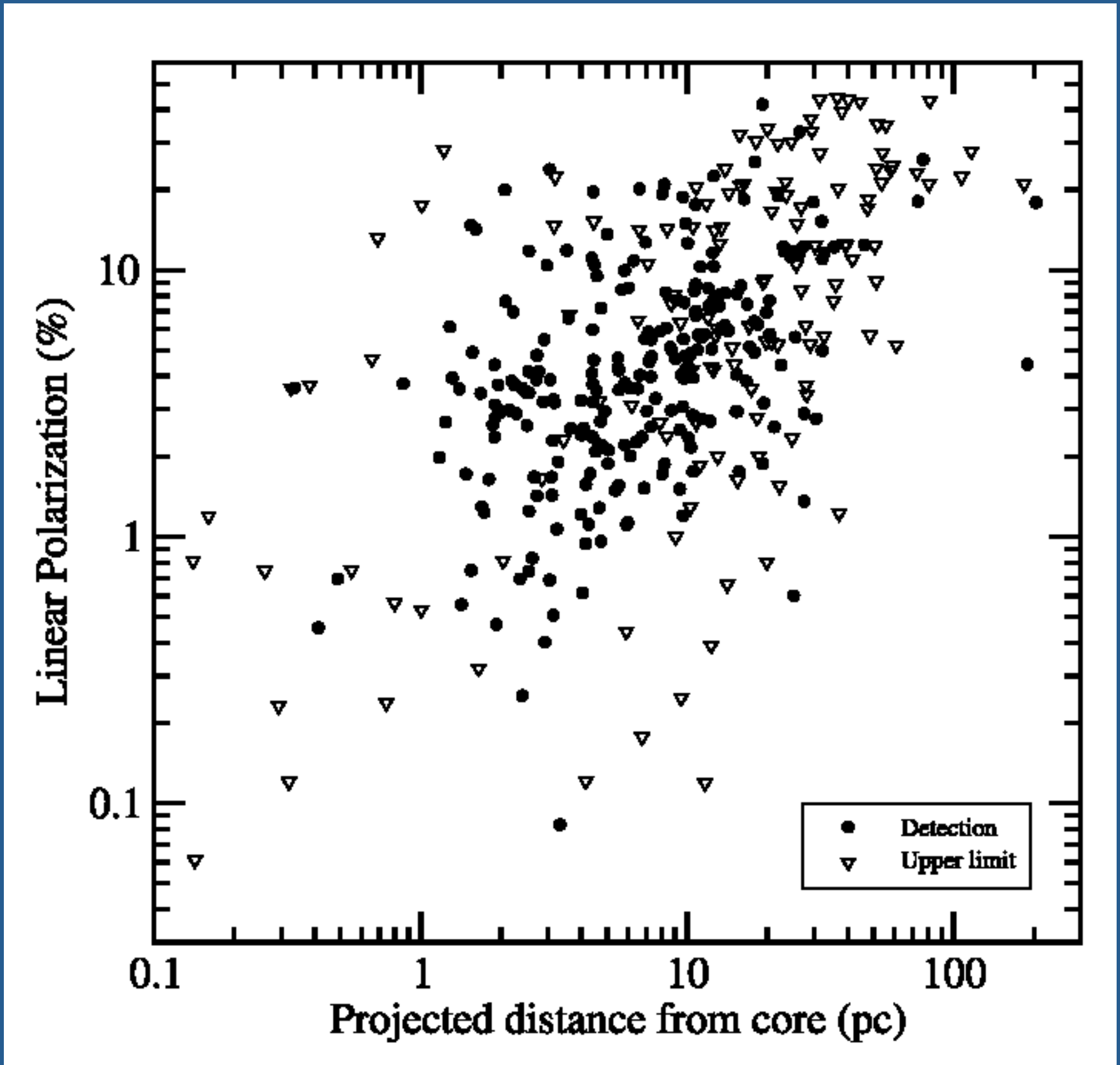
Linear Polarization (%)
Projected distance from core (pc)
Detection
Upper limit

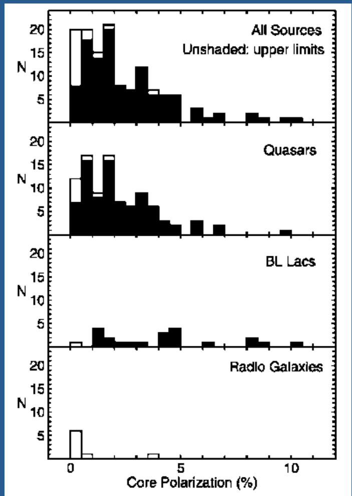
All Sources
Unshaded: upper limits
Quasars
BL Lacs
Radio Galaxies
N
Core Polarization (%)

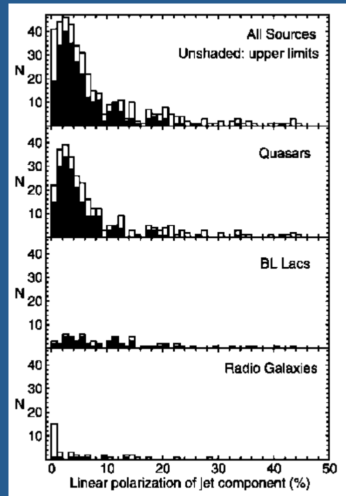
All Sources
Unshaded: upper limits
Quasars
BL Lacs
Radio Galaxies
N
Linear polarization of jet component (%)

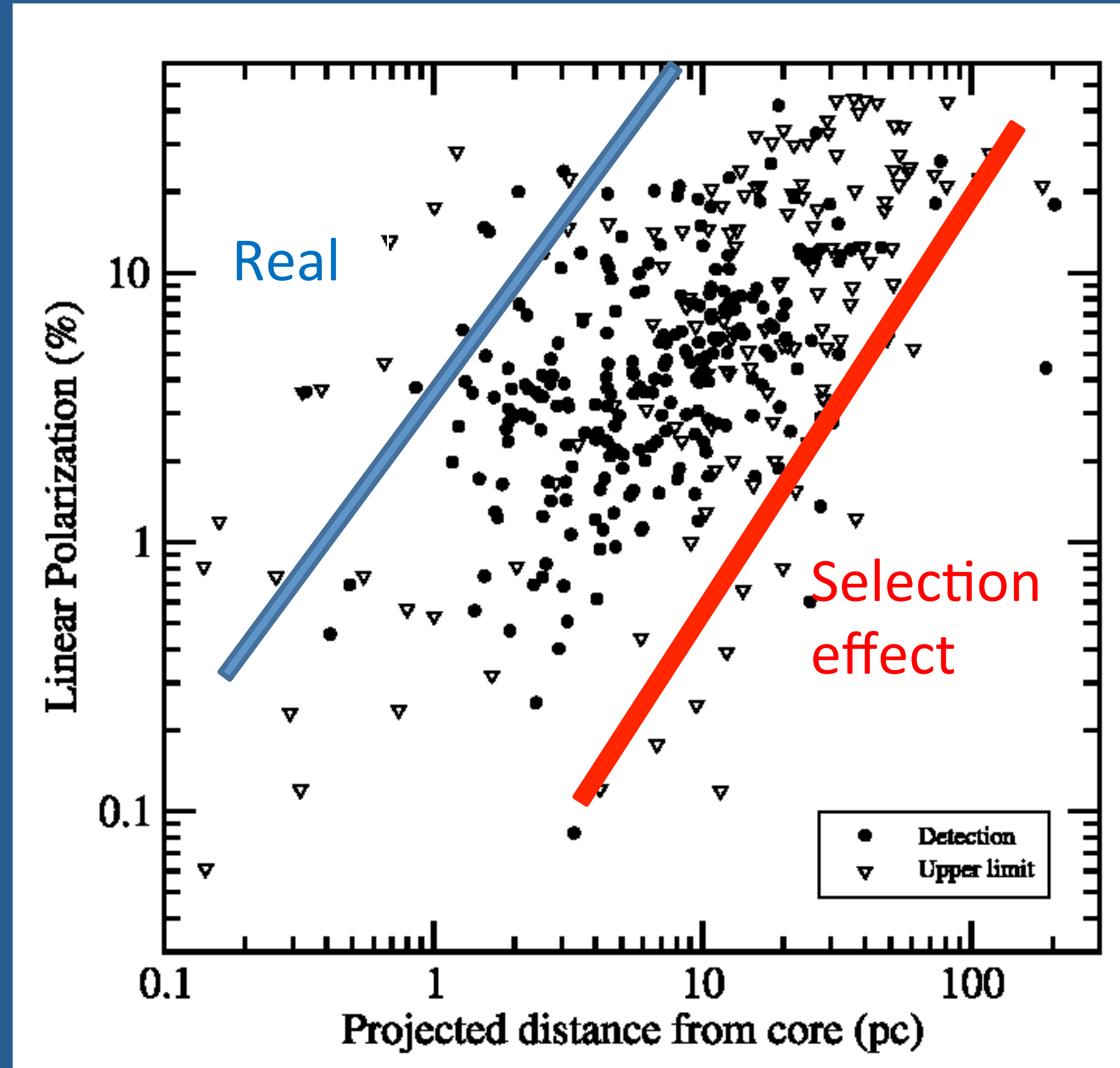
Real
Selection
effect
Linear Polarization (%)
Projected distance from core (pc)
Detection
Upper limit

Two simple field models + aberration

$$\cos\theta' = \frac{\cos\theta - \beta}{1 - \beta\cos\theta}$$

The jet makes an angle θ to the line of sight.

We "view" the magnetic field structure from an angle θ' in the rest frame of the jet.

Two simple field models + aberration

(1) Disordered field B_r
$+$ poloidal field B_p

E vectors transverse to jet

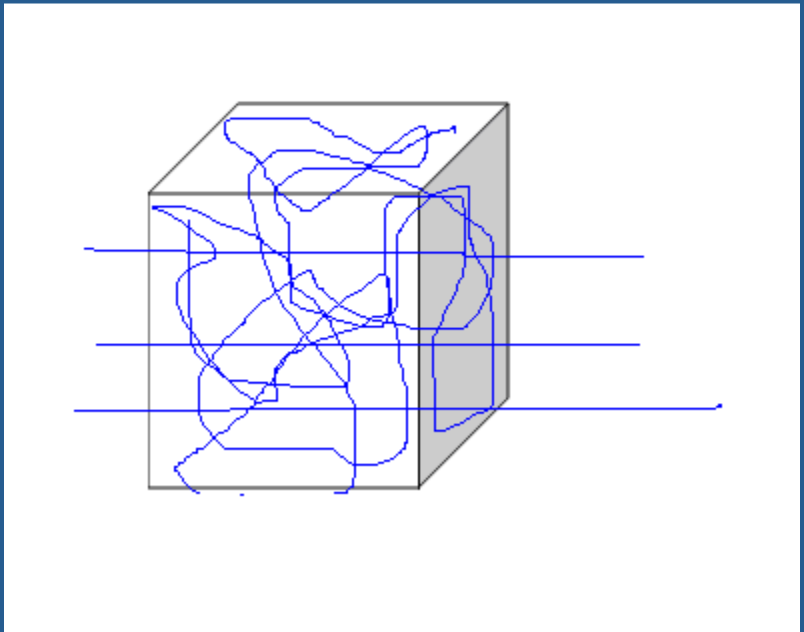

Jet direction

$$\frac{p}{p_0} = \frac{3\,\xi^2 \sin^2\theta'}{2 + 3\xi^2 \sin^2\theta'} \quad \textit{where}\ \ \xi = B_p/B_r$$

Two simple field models + aberration

(2) Disordered field compressed in one direction by a transverse shock (Laing sheet)

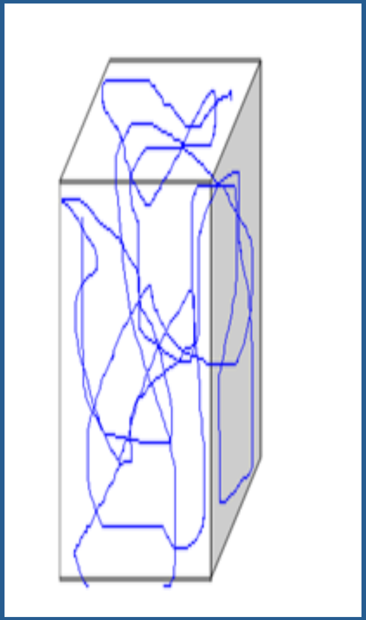

Jet direction

E vectors parallel to jet

$$\frac{p}{p_0} = \frac{-(1-k^2)\sin^2\theta'}{2-(1-k^2)\sin^2\theta'} \quad where\ k\ is\ the\ compression$$

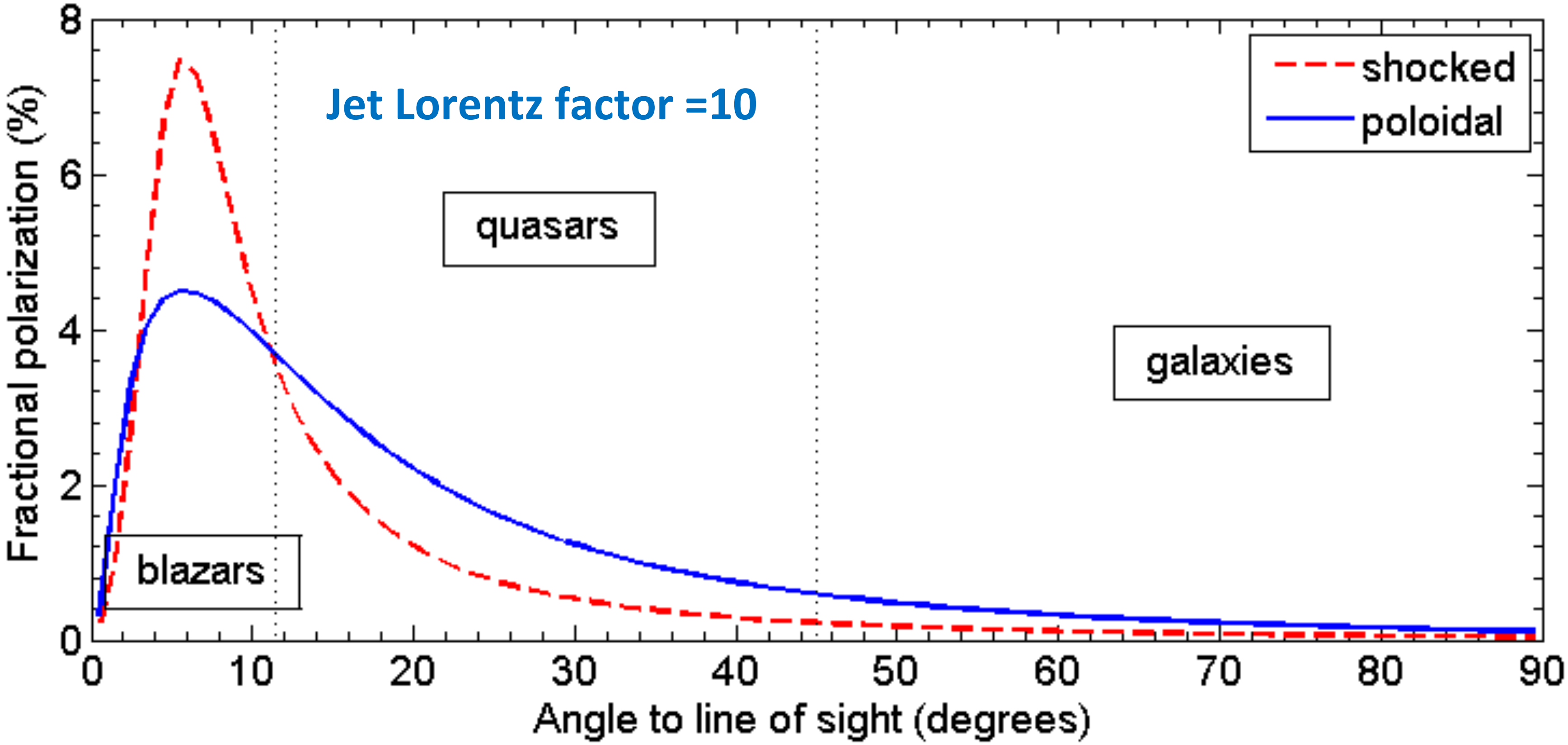

a) At $\theta = \arccos \beta = 5.7^{o}$ we view the jet from the side ($\theta' = 90^{o}$), giving peak polarization.

b) For 'galaxies' we are looking almost straight down the jet ($\theta' > 166^{o}$), and we see mostly the tangled field.

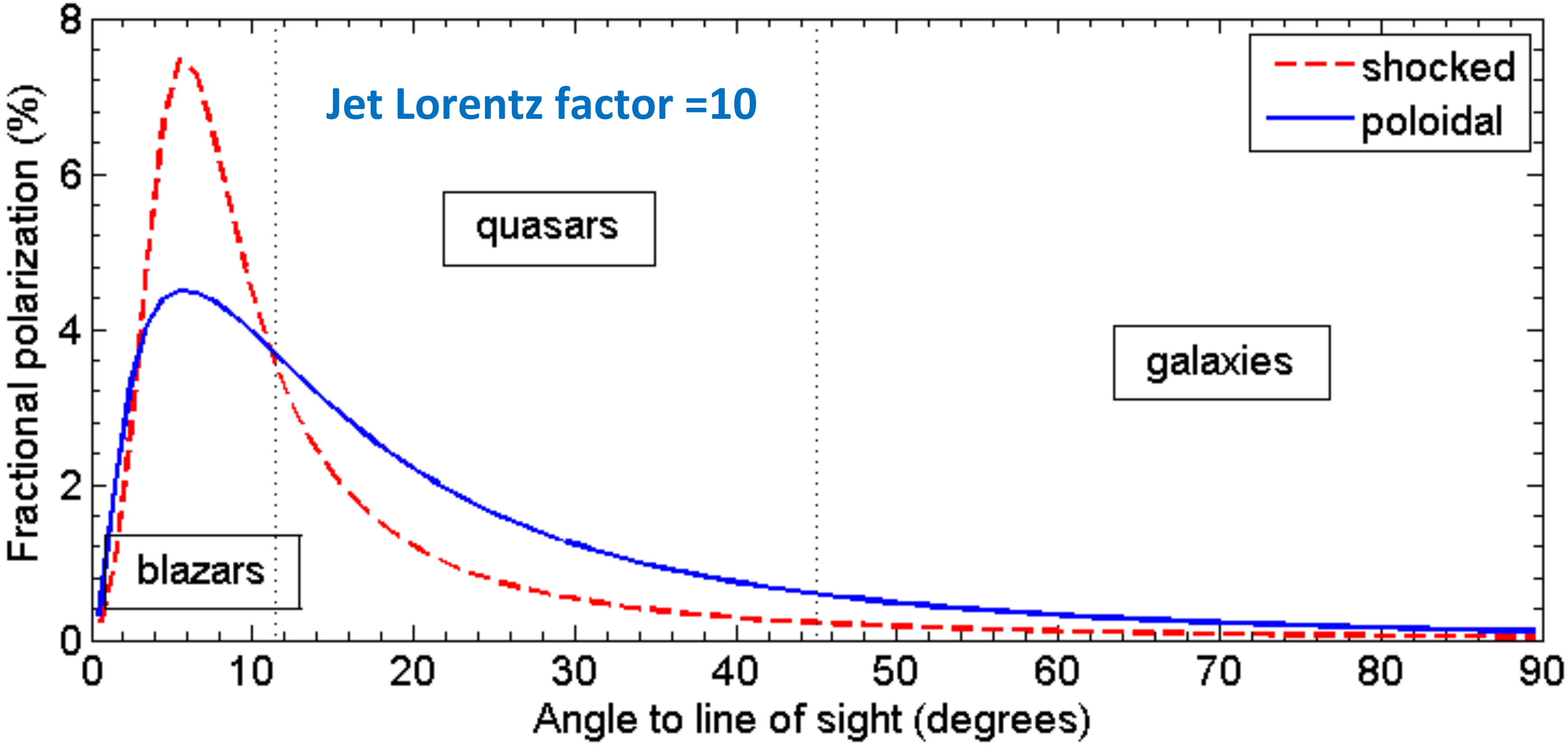

c) Aberration is crucial for interpreting polarization observations.

d) Galaxies may suffer additional depolarization in the obscuring torus, but it is probably not required.

2) EVPA-jet PA alignment (5 GHz)

2) EVPA-jet PA alignment (5 GHz)

cores

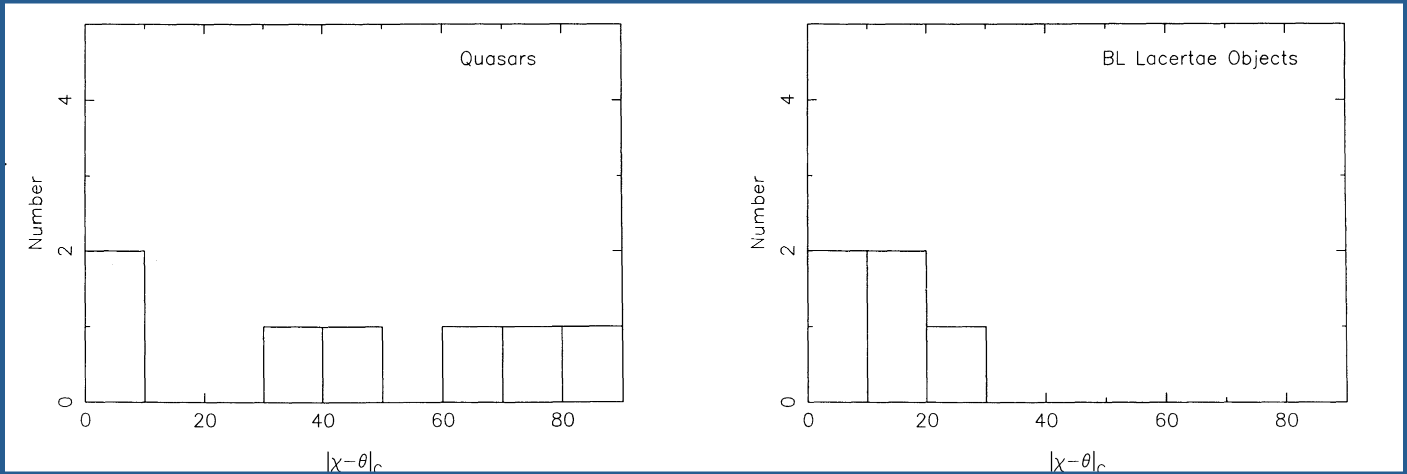

jet features

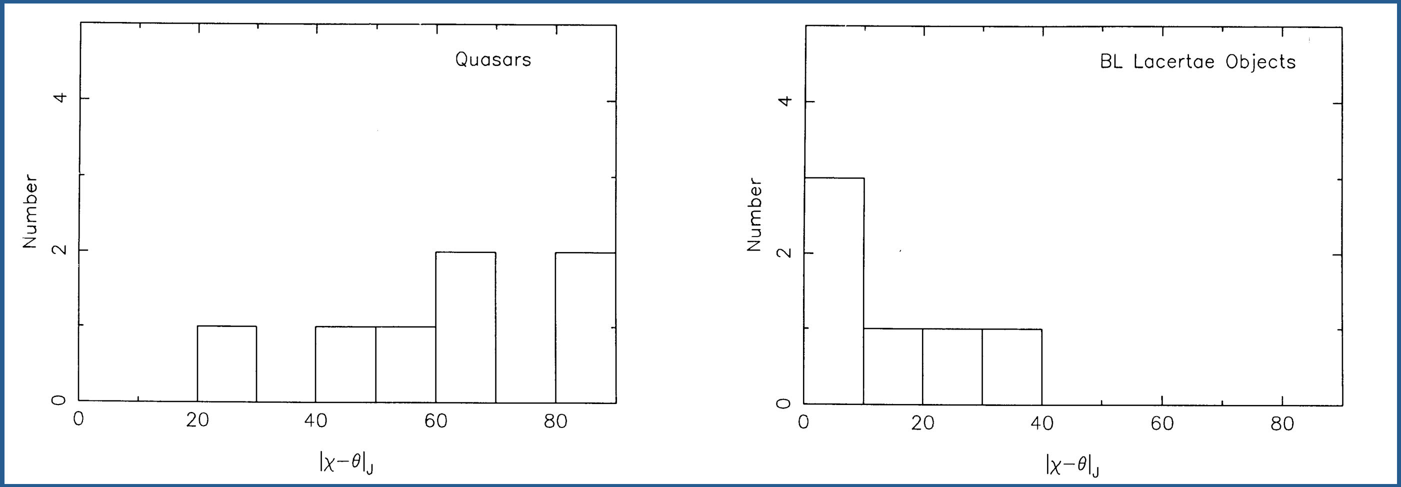

Cawthorne et al. 1993

2) EVPA-jet PA alignment (15 GHz)

cores

jet features

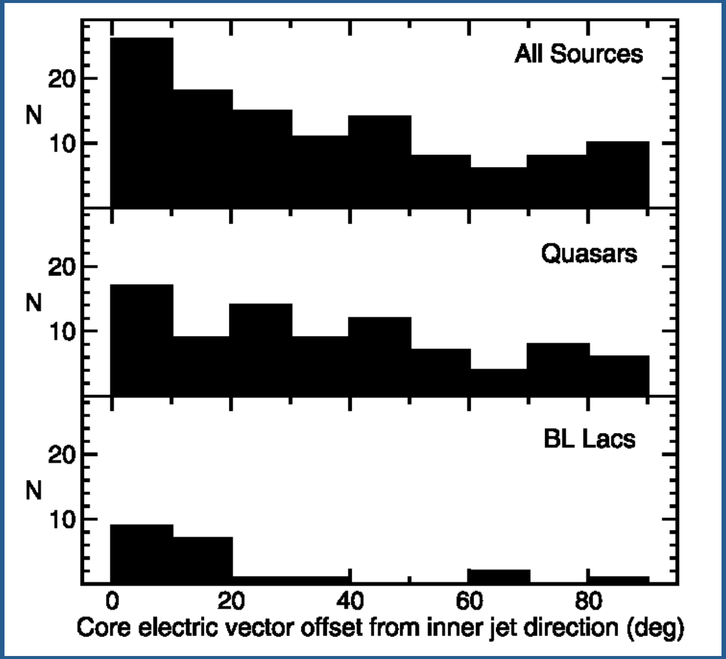

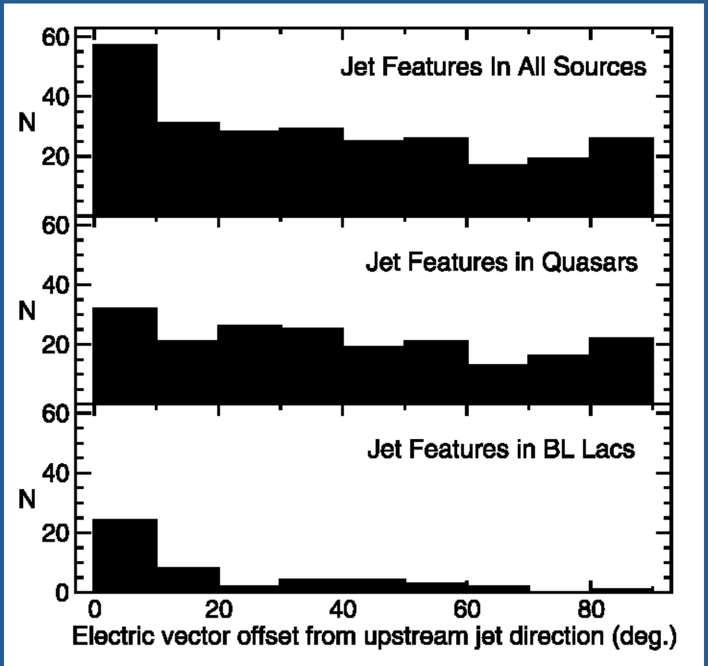

Lister & Homan 2005

2) EVPA-jet PA alignment (43 GHz)

cores

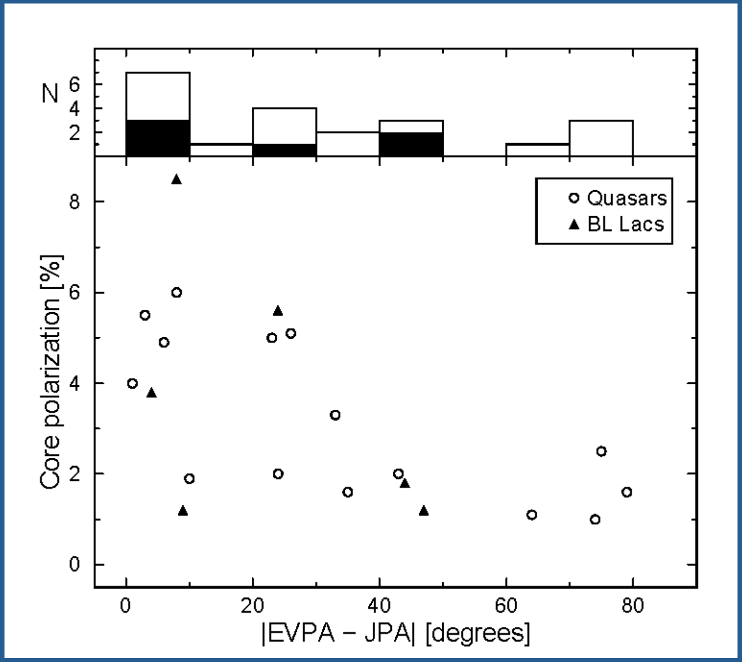

jet features

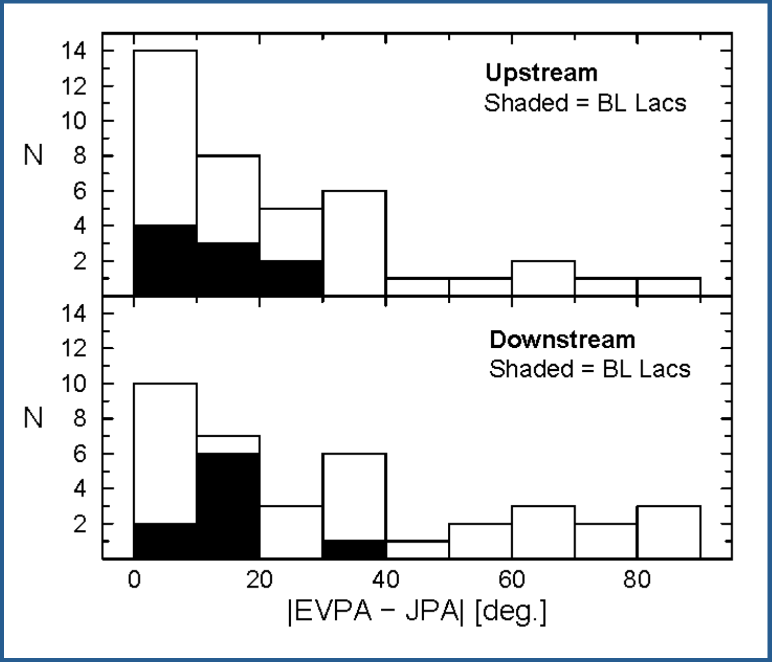

Lister 2001

3) Two possible models for misaligned EVPAs

a) Oblique shocks

b) Differential Doppler effect in a conical jet

3a) Oblique shocks?

Jump conditions:

$$\beta_d(par) = \beta_u(par)$$

$$\beta_d(perp) \times \beta_u(perp) = \frac{1}{3}$$

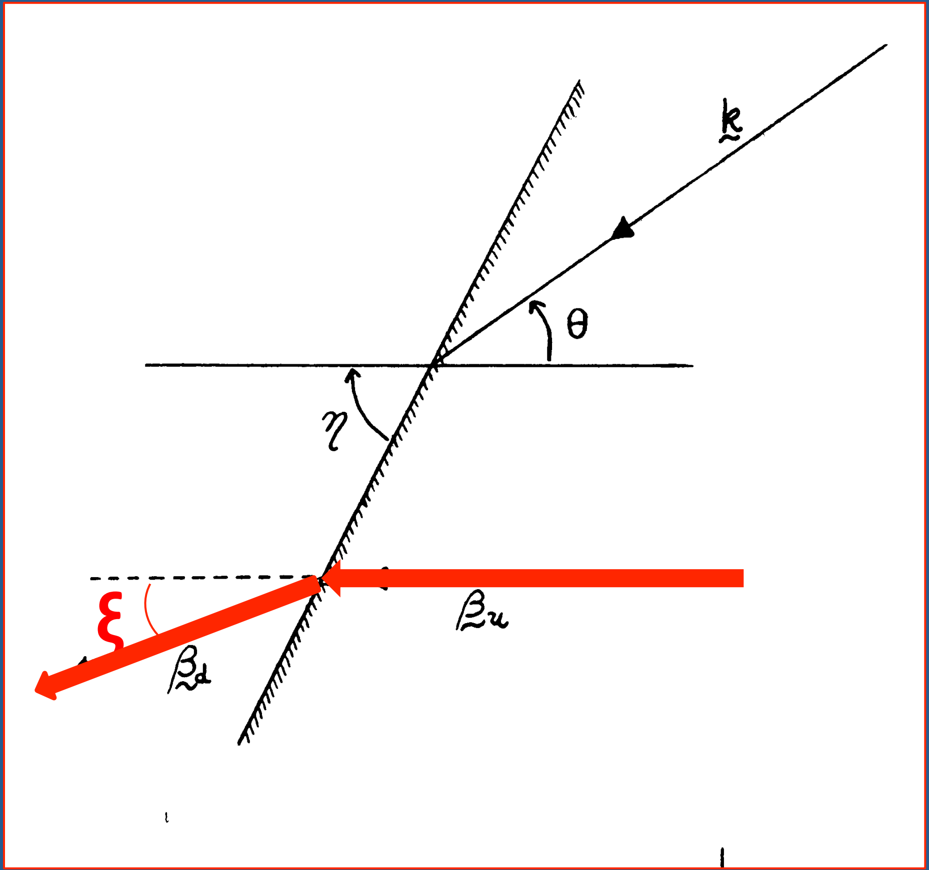

ξ, the deflection angle is given by

$$\tan\,\xi = \frac{\tan^2\,\eta(3\beta_u^2 - 1) - (1 - \beta_u^2)}{\tan\,\eta(\tan^2\,\eta + 1 + 2\beta_u^2)}$$

Lind & Blandford 1985
Cawthorne & Cobb 1990
Bicknell & Begelman 1996
Cawthorne 2006

3b) Differential Doppler effect in a conical jet?

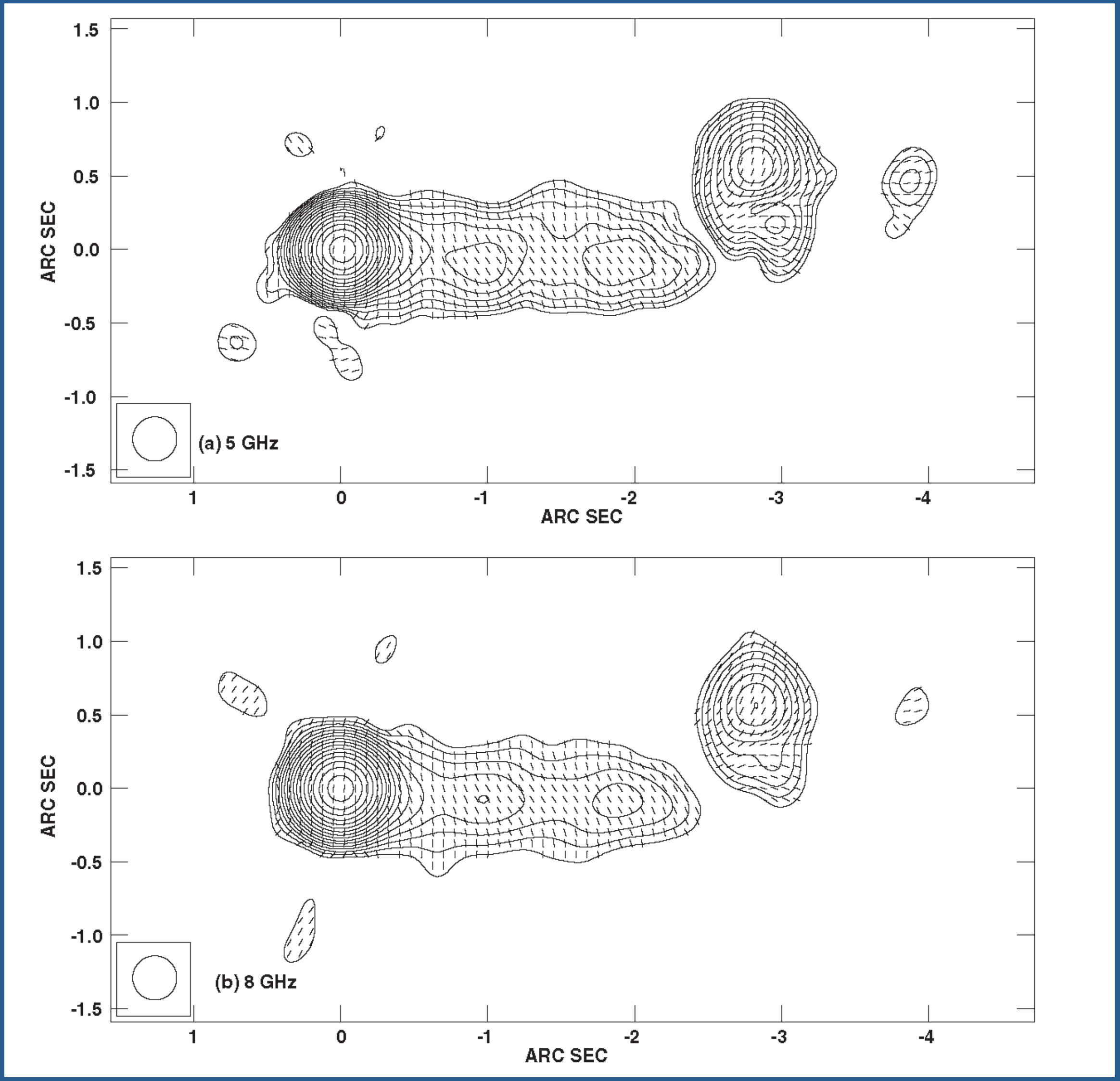

VLA images of 3C 345:

<-- 5 GHz

<-- 8GHz

3b) Differential Doppler effect in a conical jet?

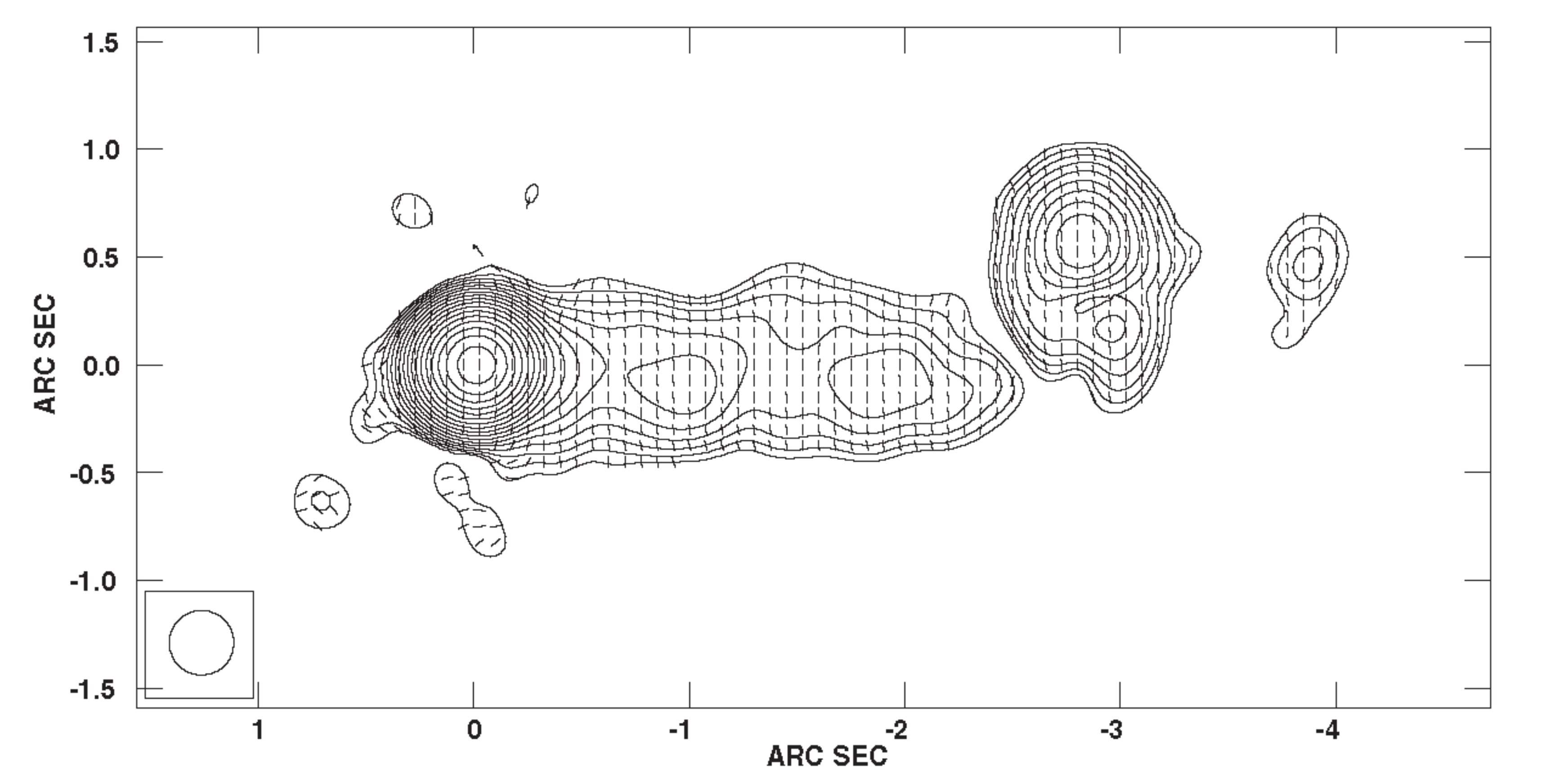

Tick marks are oriented at EVPA (5 GHz) – EVPA (8 GHz)

3b) Differential Doppler effect in a conical jet?

i. In a cylindrical jet, a helical field exhibits an EVPA of 0^o or 90^o, depending on the pitch angle. (Stokes U from the back half of the jet and Stokes U from the front half of the jet cancel.)

3b) Differential Doppler effect in a conical jet?

i. In a cylindrical jet, a helical field exhibits an EVPA of 0^o or 90^o, depending on the pitch angle. (Stokes U from the back half of the jet and Stokes U from the front half of the jet cancel.)

ii. In a conical jet at a small angle to the line of sight, the difference in Doppler factors between the front and the back of the jet breaks the cancellation, Stokes U is no longer zero, and the EVPAs appear "twisted."

3b) Differential Doppler effect in a conical jet?

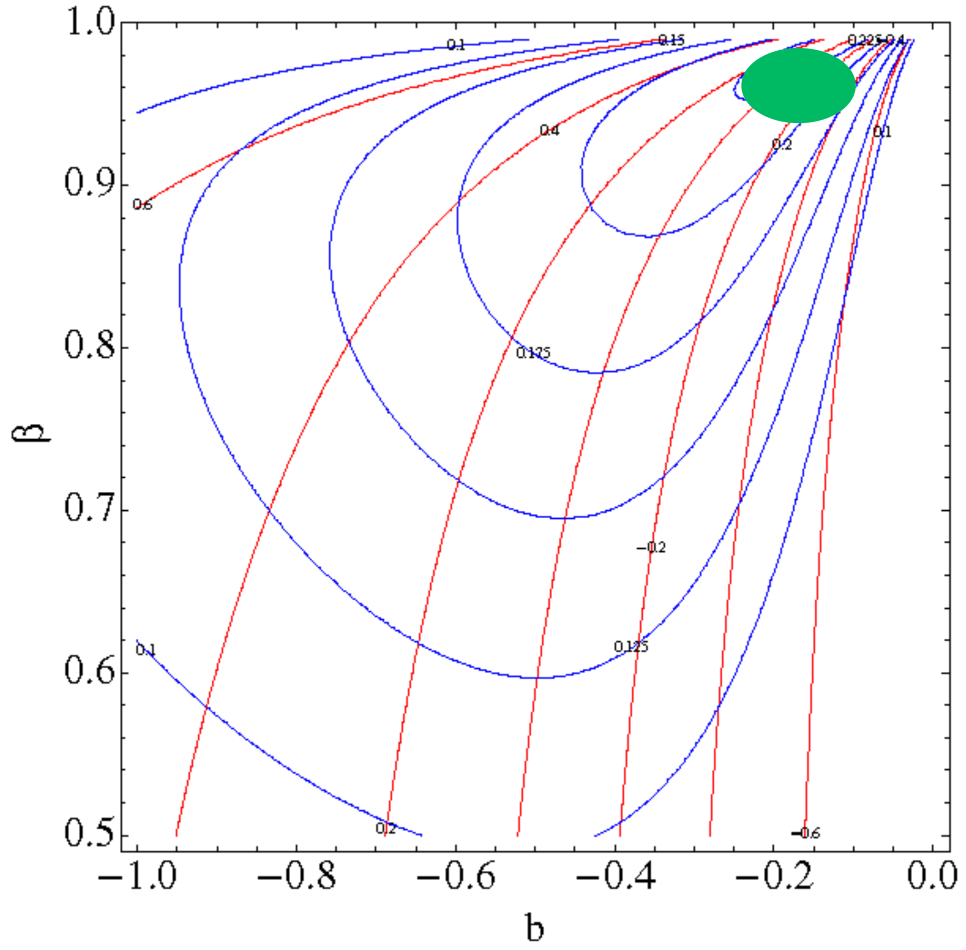

Figure 3. Model curves of constant Q/I (red,) and U/I (blue) at the center of the jet, as functions of the parameters b and β, assuming $\phi_a = 9\overset{\circ}{.}4$.

Toroidal field is generated by a uniform current density.

Add a uniform poloidal field.

$b = B_{pol}/B_{tor}$ at surface.

observed opening angle = 9.4°

The green spot marks the region of acceptable models

Roberts & Wardle 2012

3b) Differential Doppler effect in a conical jet?

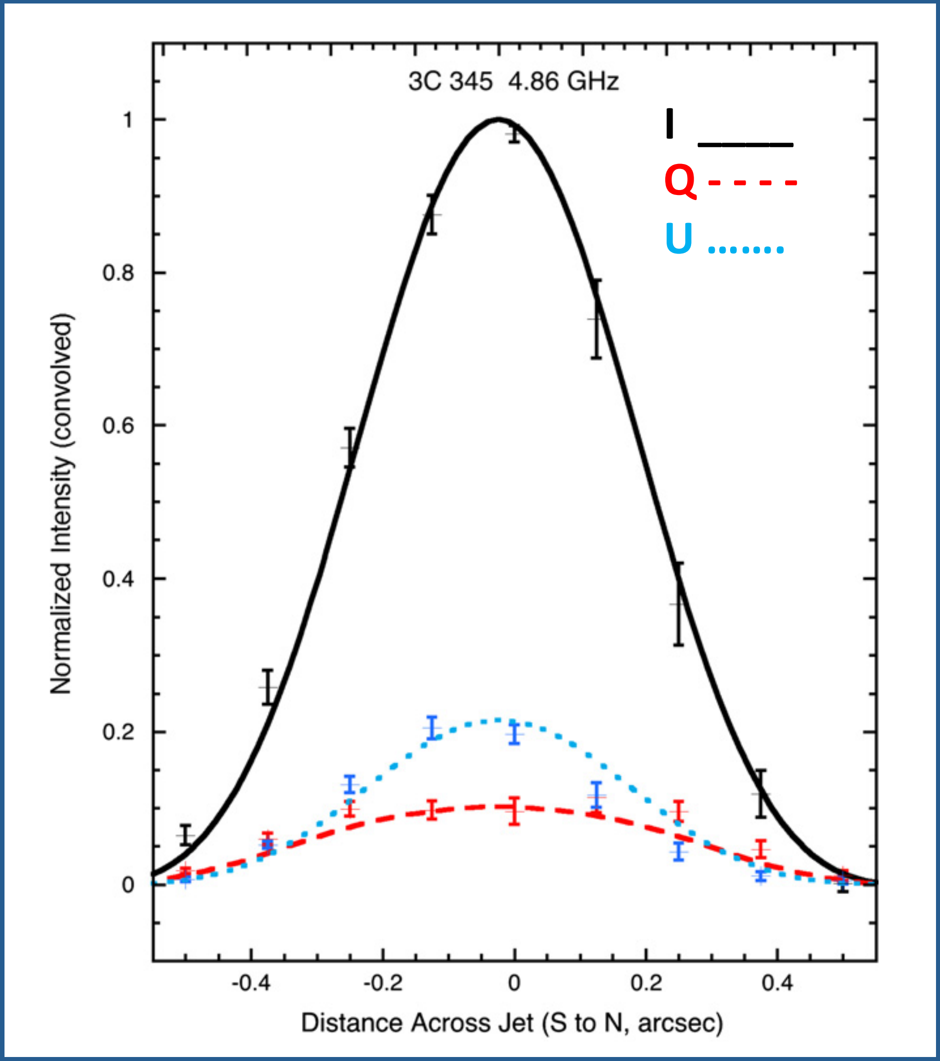

Nominal model:

B_{pol}/B_{tor} at surface = -0.19

$\beta = 0.97$ ($\Gamma = 4.1$)

Observed opening angle = 9.4°
intrinsic opening angle = 2.3°

<u>In general, this is a way of breaking the symmetry in an axisymmetric jet, and could be applied on parsec scales too.</u>

Roberts & Wardle 2012

4) Radio core EVPA - optical EVPA alignment

4) Radio core EVPA - optical EVPA alignment

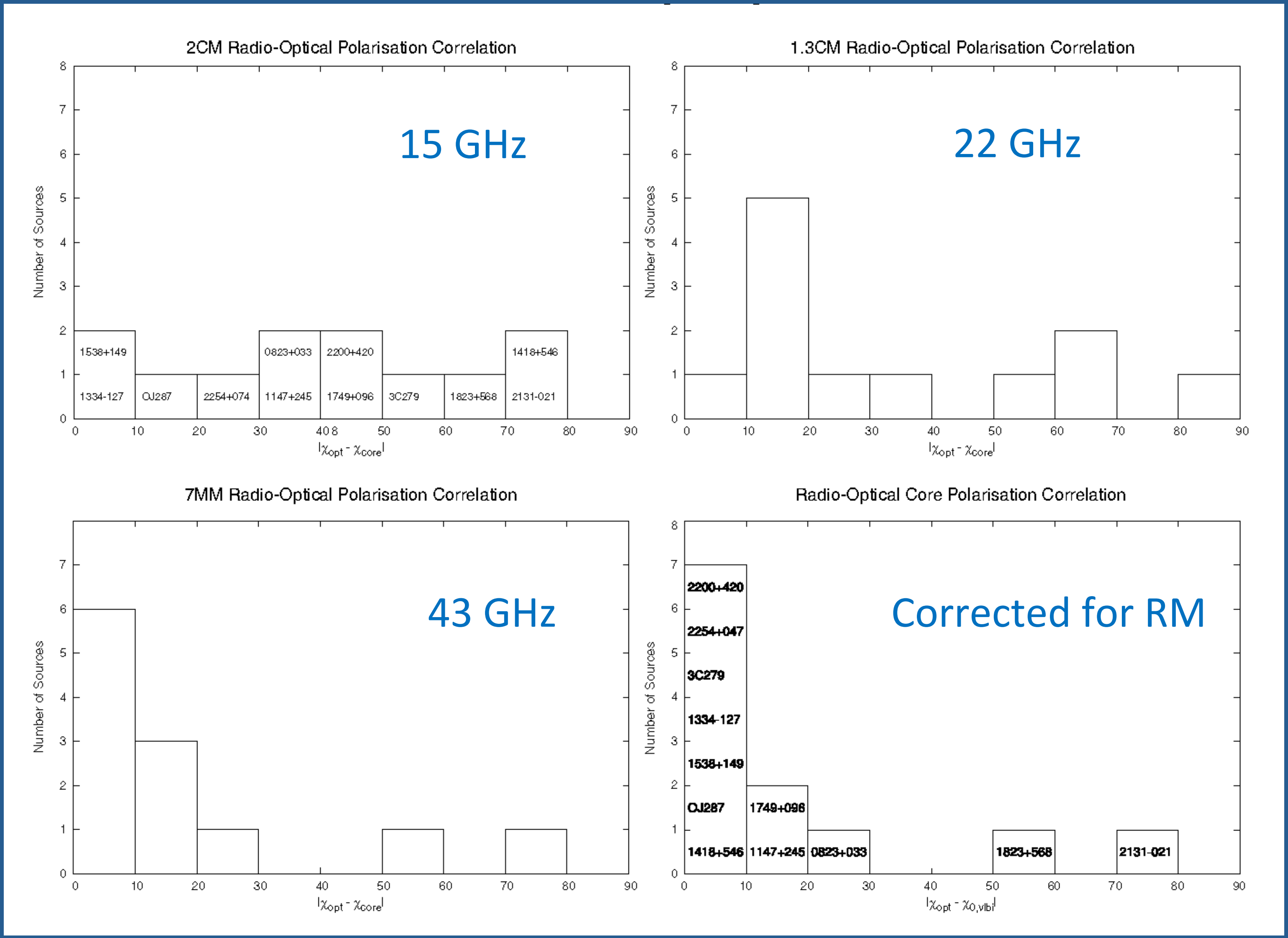

Gabuzda et al. 2006 (mainly BL Lac objects)

5) Optical polarization

Correlated changes would be strong evidence for co-spatial emission regions.

5) Optical polarization

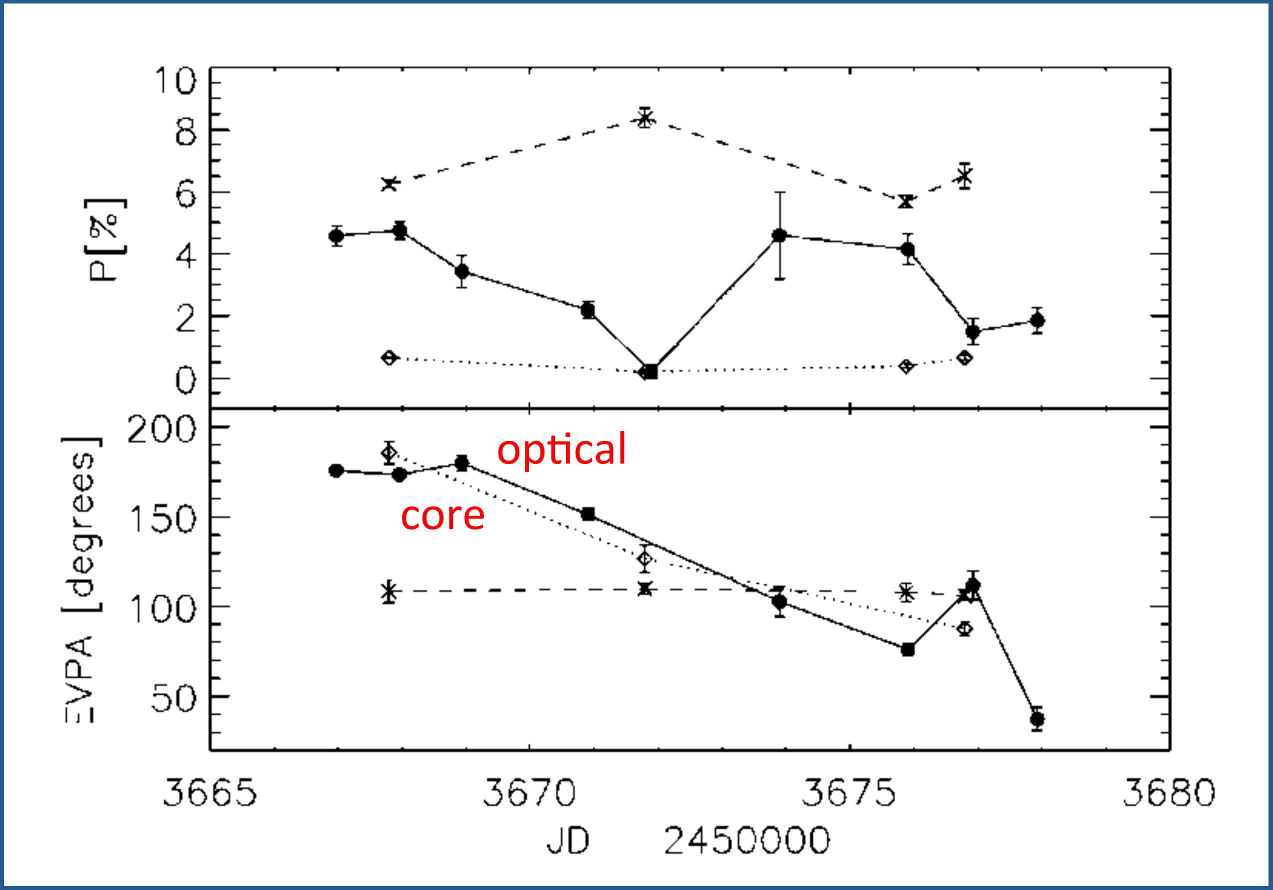

PKS 0420-014

continuous line = optical (450-750 nm)

dotted line = 43 GHz "pseudocore"

dashed line = 43 GHz first jet component

D'Arcangelo et al. 2007 also 0836+710, Jorstad, this meeting, and Troitskiy, poster #34

5) Optical polarization

PKS 1510-089 Marscher et al. 2010

In 2009, the optical EVPA rotated 720° just prior to a spike in flux and fractional polarization, AND a gamma-ray outburst AND the launch of a new VLBI component.

Similar behaviour is seen in other sources, e.g. 3C454.3 (Marscher, this meeting), also PKS 1510-089 in 2011 (Orienti, this meeting).

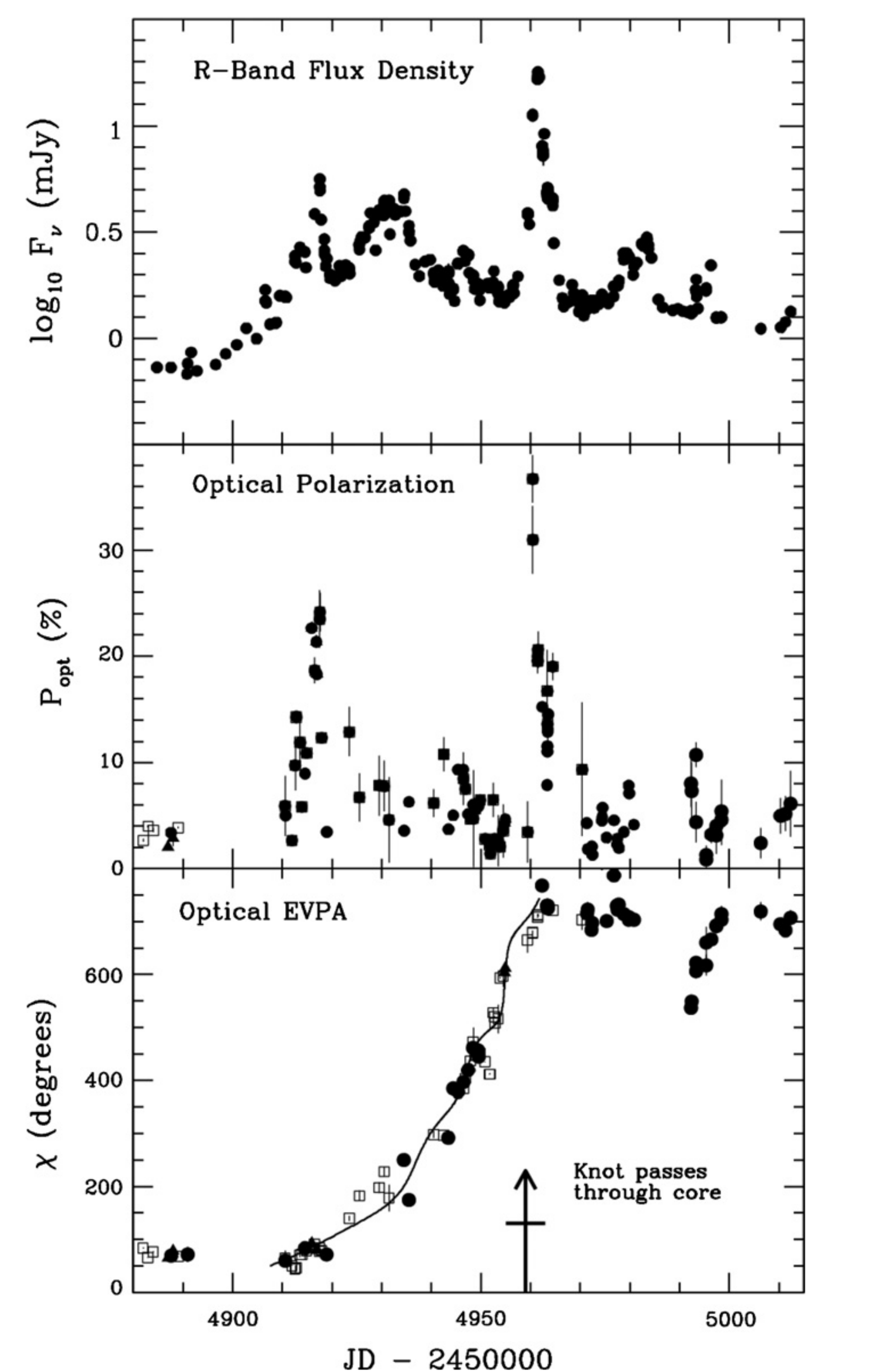

5) Optical polarization

PKS 1510-089 Marscher et al. 2010

Model from Marscher et al. 2005

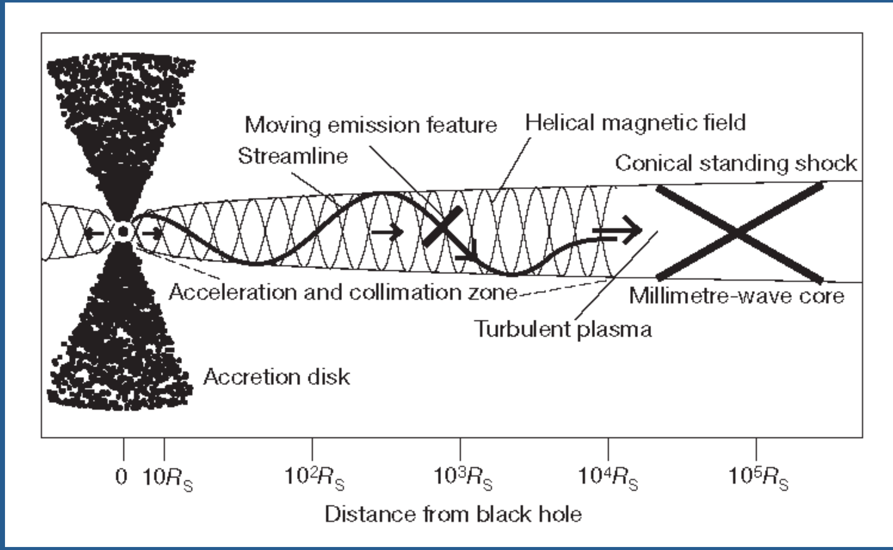

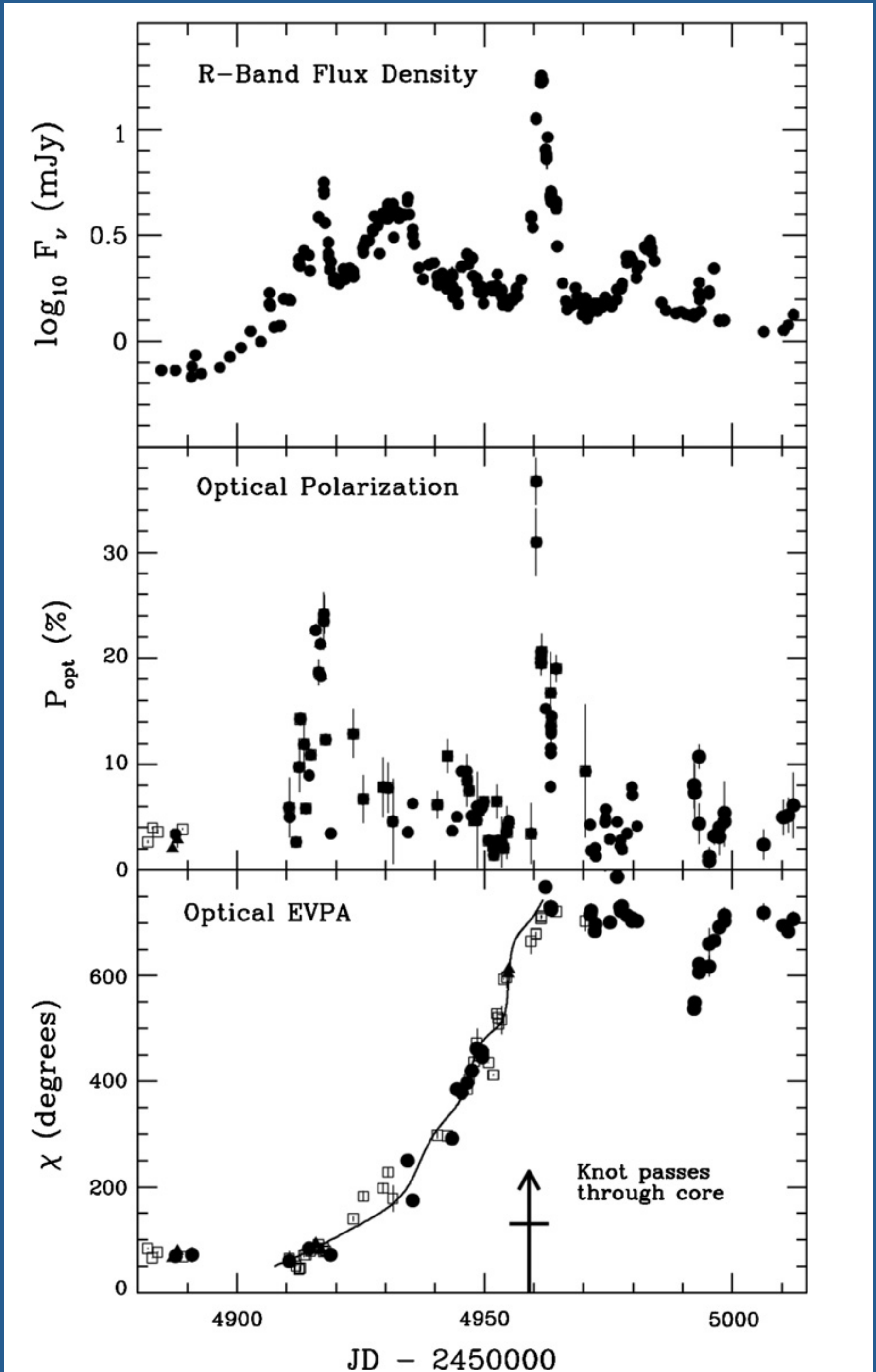

Many features of this model are very plausible. Almost impossible to get here without multi-wavelength, close-spaced monitoring and imaging.

6) Rotation Measures

6) Rotation Measures

Zavala & Taylor 2004, peering through "Faraday's Fog"

PKS 0458-020
8-15 GHz

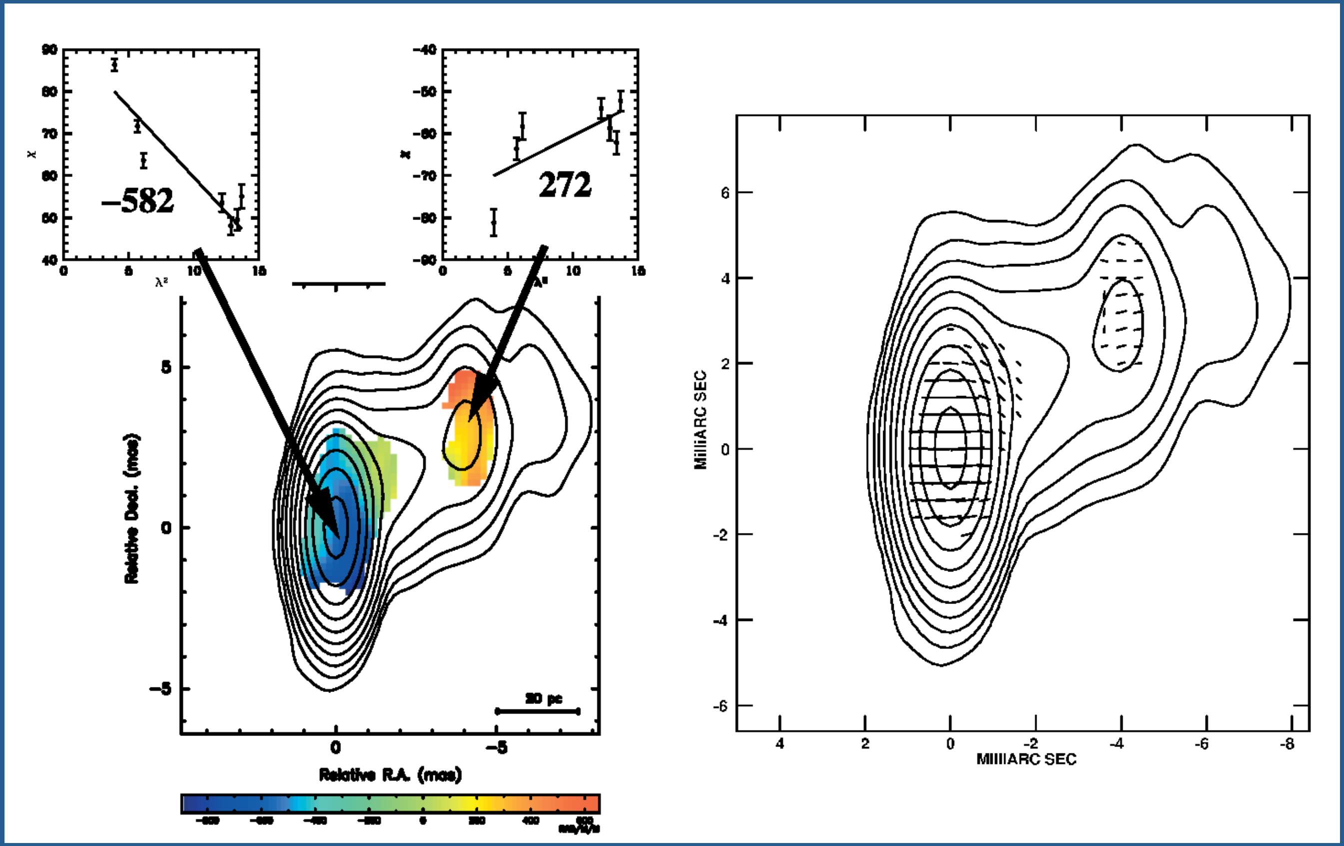

6) Rotation Measures

Hovatta et al 2012

PKS 0458-020
8-15 GHz

Note how they solve the problem of how to show error bars on a false color image.

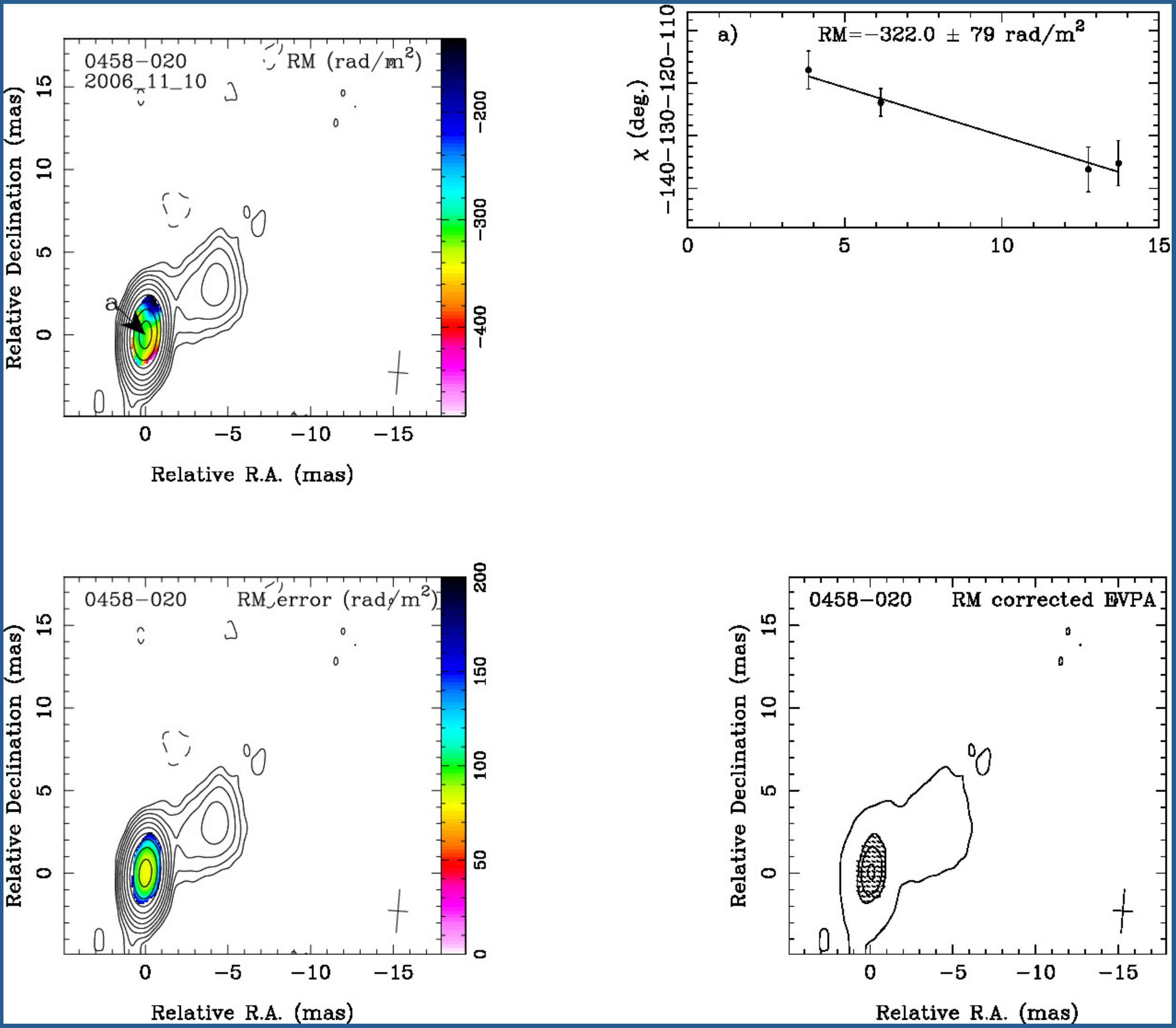

6) Rotation Measures

Hovatta et al 2012
8-15 GHz

Very few RMs are > 1000 rad/m^2 .
(This corresponds to 23^o EVPA rotation at 15 GHz, which is not enough to align the EVPAs with the jet direction. But see Lister, next talk.)

Cores have bigger RMs than jets.

Quasars have bigger RMs than BL Lac objects

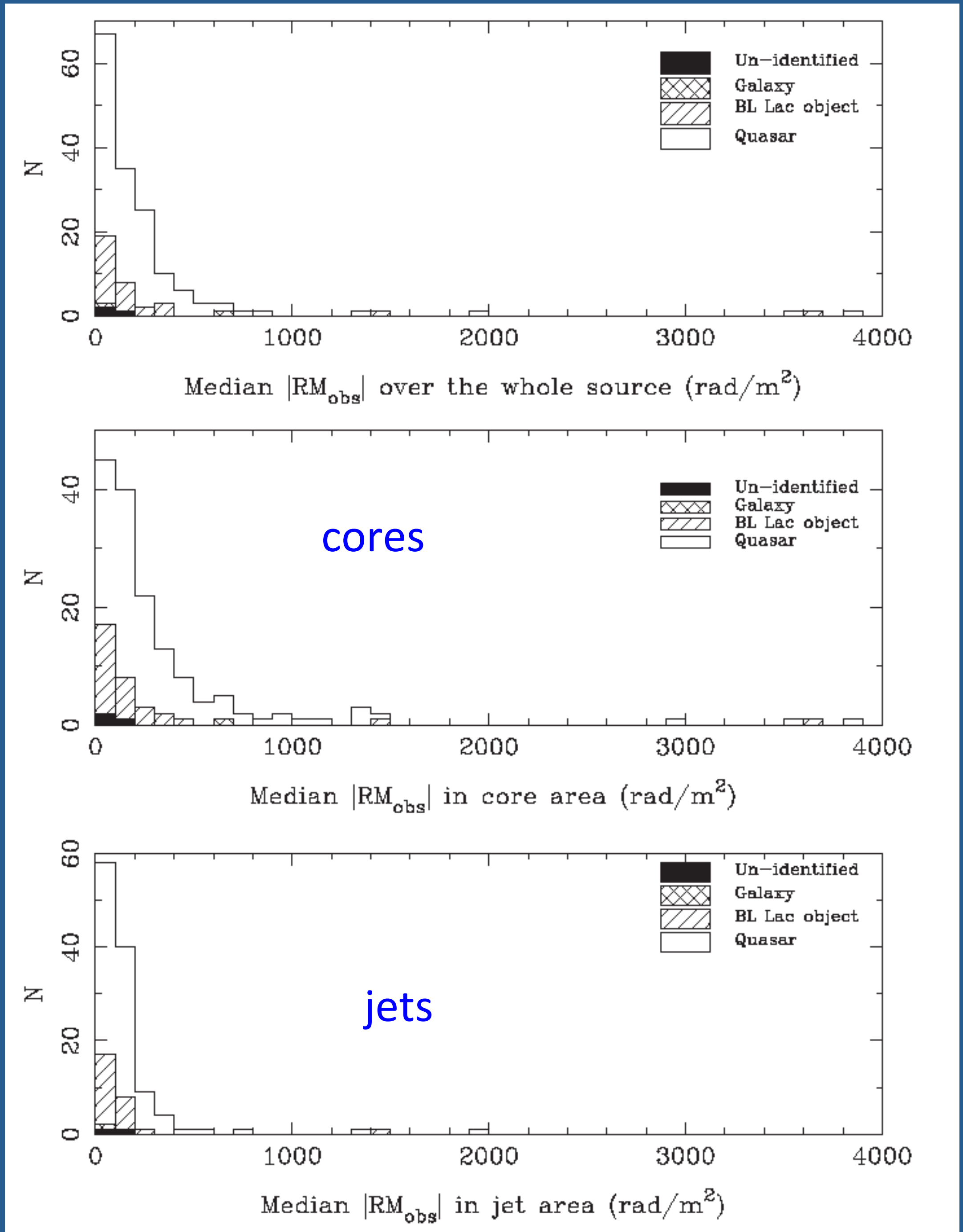

6) Rotation Measures

Algaba, Gabuzda & Smith 2012
12-43 GHz

Core RMs are much higher at higher frequencies.

For a Blandford-Königl jet, the distance of the $\tau = 1$ surface from the apex of the jet ~ λ.

It is very plausible that at higher frequencies the lines of sight go through regions of higher density and magnetic field

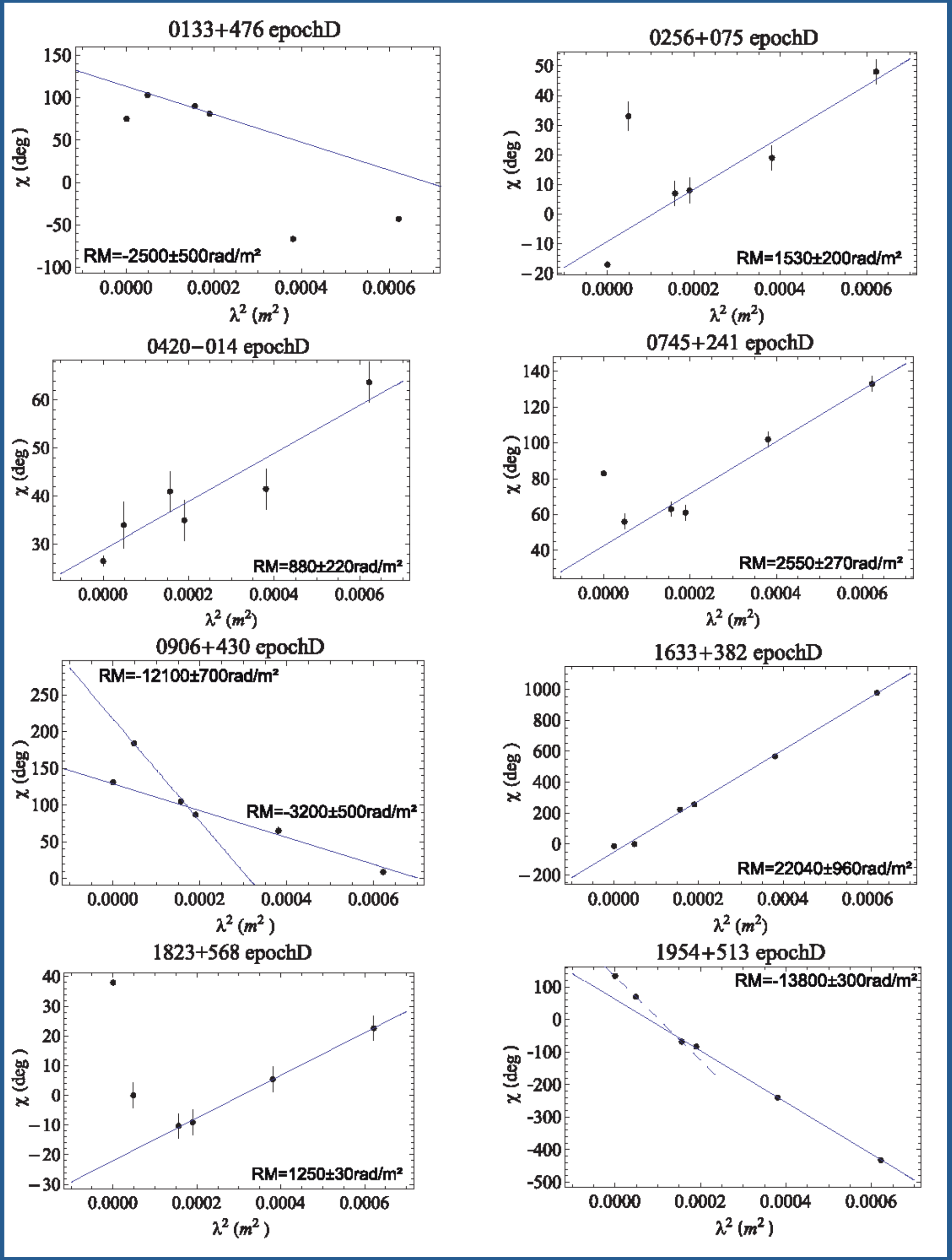

6) Rotation Measures

The cores clearly contain complex Faraday screens which it may not be possible to resolve spatially.

This may be a good place to try wide band Faraday synthesis:

Original idea: Burn 1966
Resuscitated by Brentjens & de Bruyn 2005

6) Rotation Measures

The cores clearly contain complex Faraday screens that may not be possible to resolve spatially.

This may be a good place to try wide band Faraday synthesis:

Original idea: Burn 1966
Resuscitated by Brentjens & de Bruyn 2005

Illustrated by ATCA observations of PKS B 1610-771, an unresolved, 3 Jy, z=1.71 quasar,
using a 2 GHz instantaneous bandwidth from 1.1 – 3.1 GHz

O'Sullivan et al 2012

6) Rotation Measures - Faraday synthesis

First model: single RM component. Reduced χ^2= 97.3

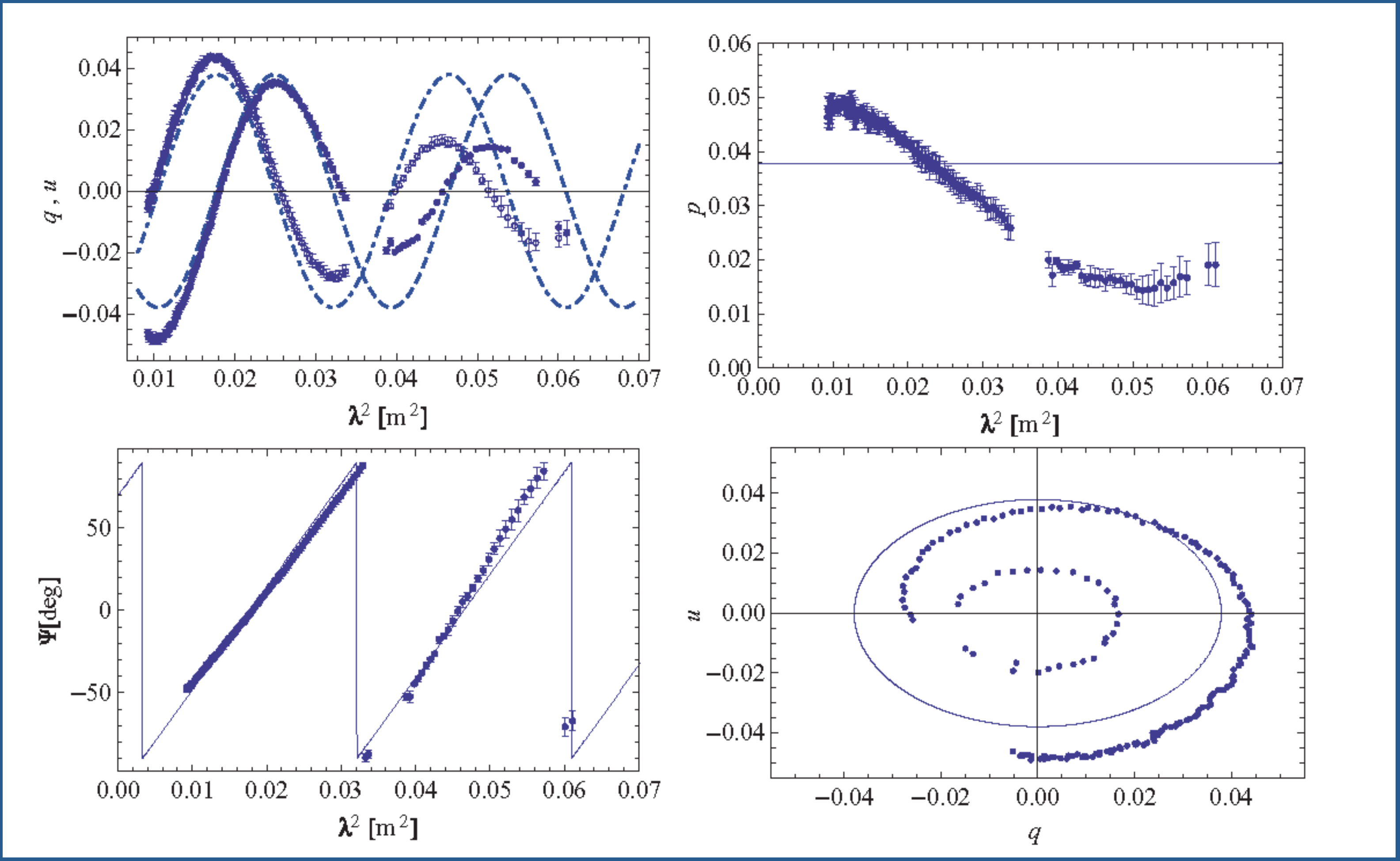

6) Rotation Measures - Faraday synthesis

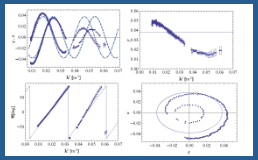

Second model: single RM component plus a Burn-type depolarizing screen. Reduced χ^2= 1.41

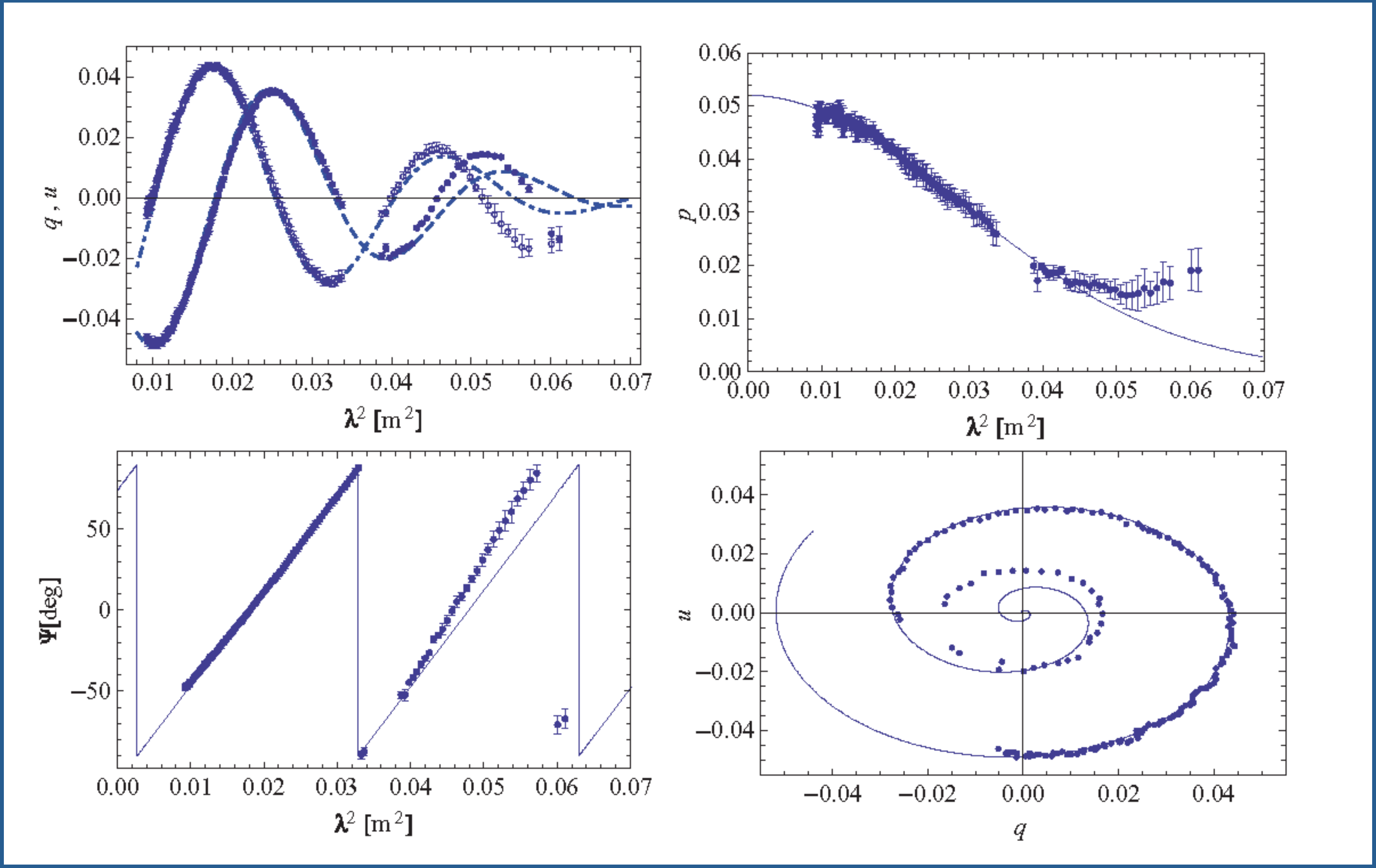

6) Rotation Measures - Faraday synthesis

Final model: two components with different polarizations and rotation measures, (107 and 78 rad/m^2). Reduced χ^2= 1.04

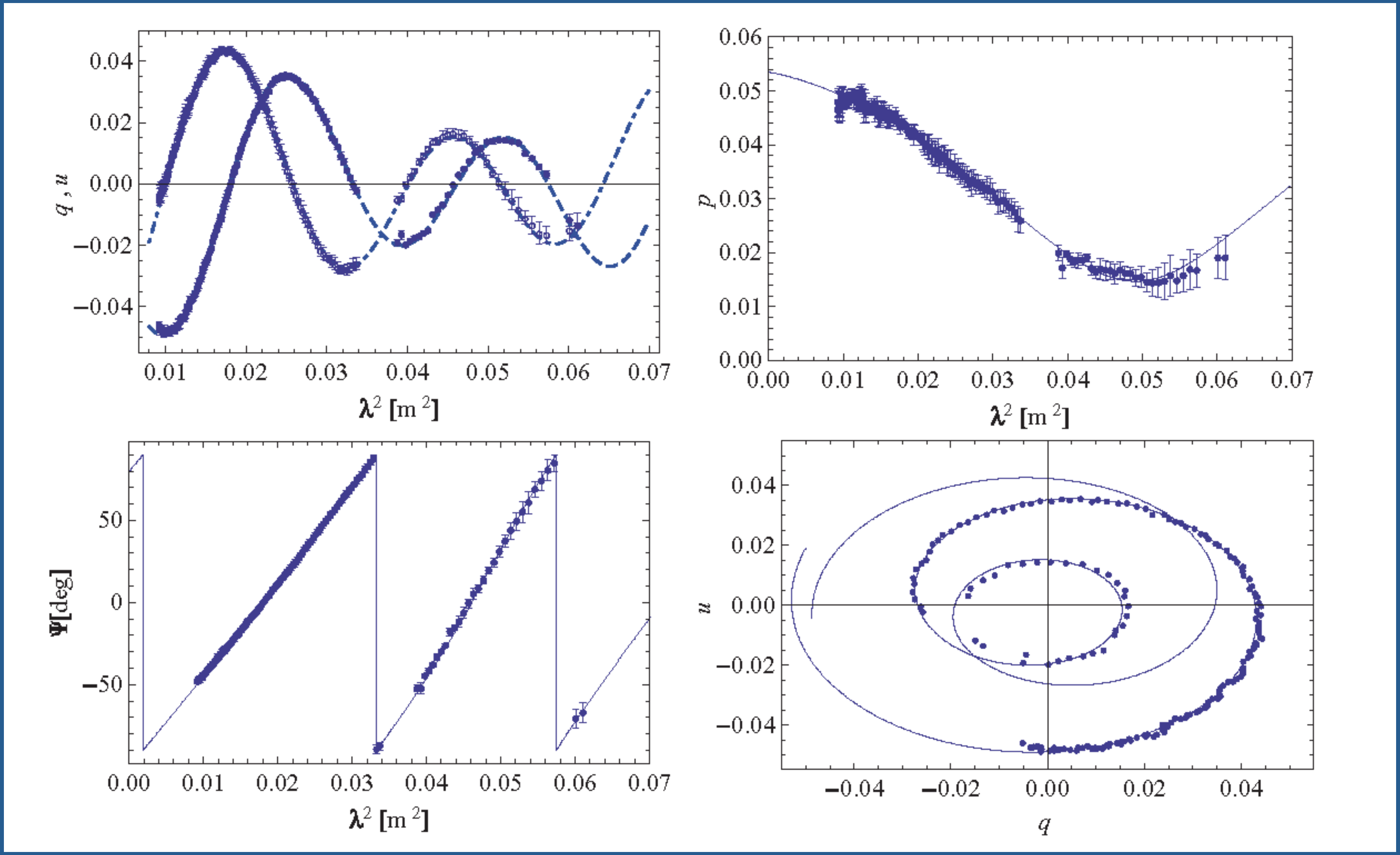

6) Rotation Measures: 3C120 (Gomez et al. 2008)

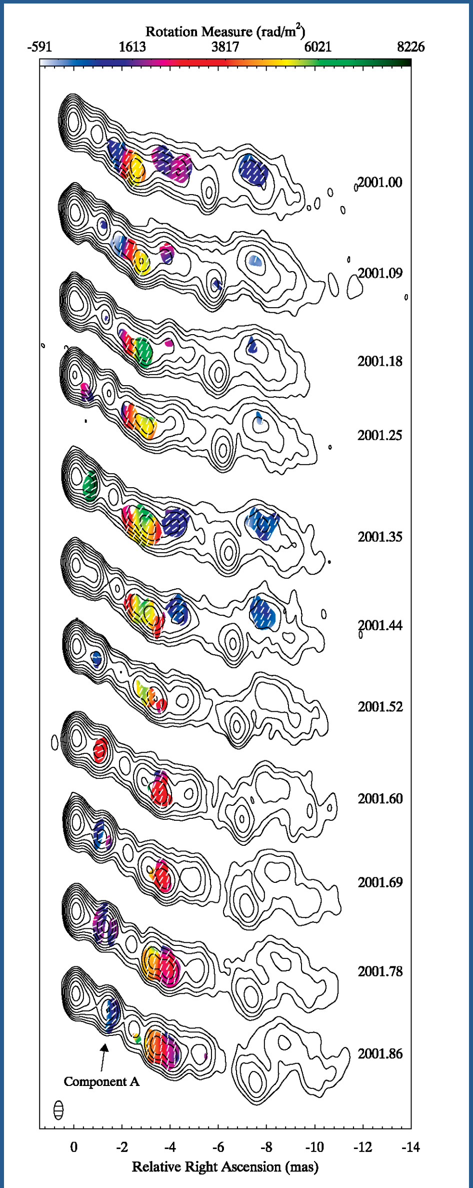

Observations at 15, 22 and 43 GHz, between 2001.00 and 2001.86

Clearly there is some variability in the small scale Rotation Measure structure.

6) Rotation Measures: 3C120 (Gomez et al. 2008)

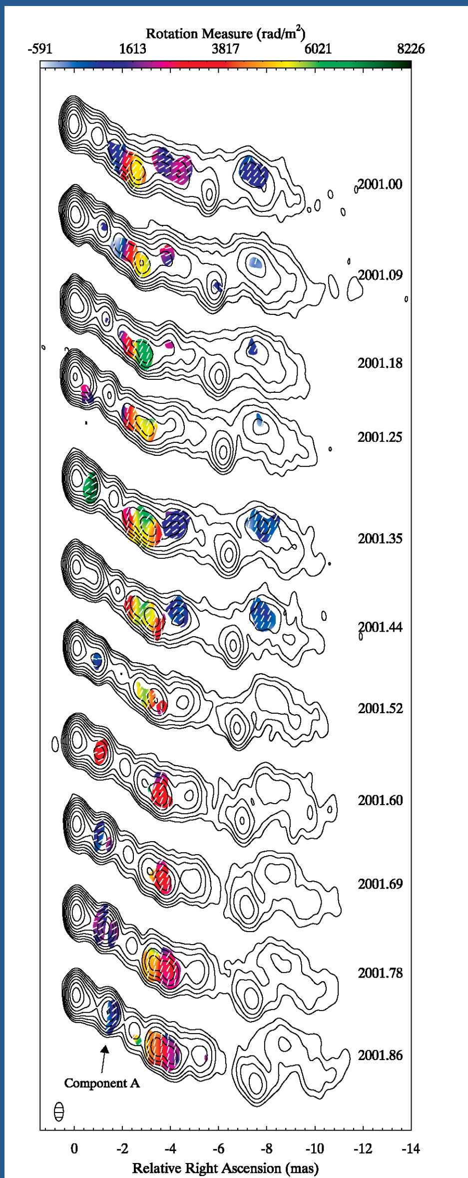

Average of all 11 RM maps together. Note the green patch of very high RM, and the transverse gradient next to it.

Note also that the magnetic field direction is everywhere aligned with the jet.

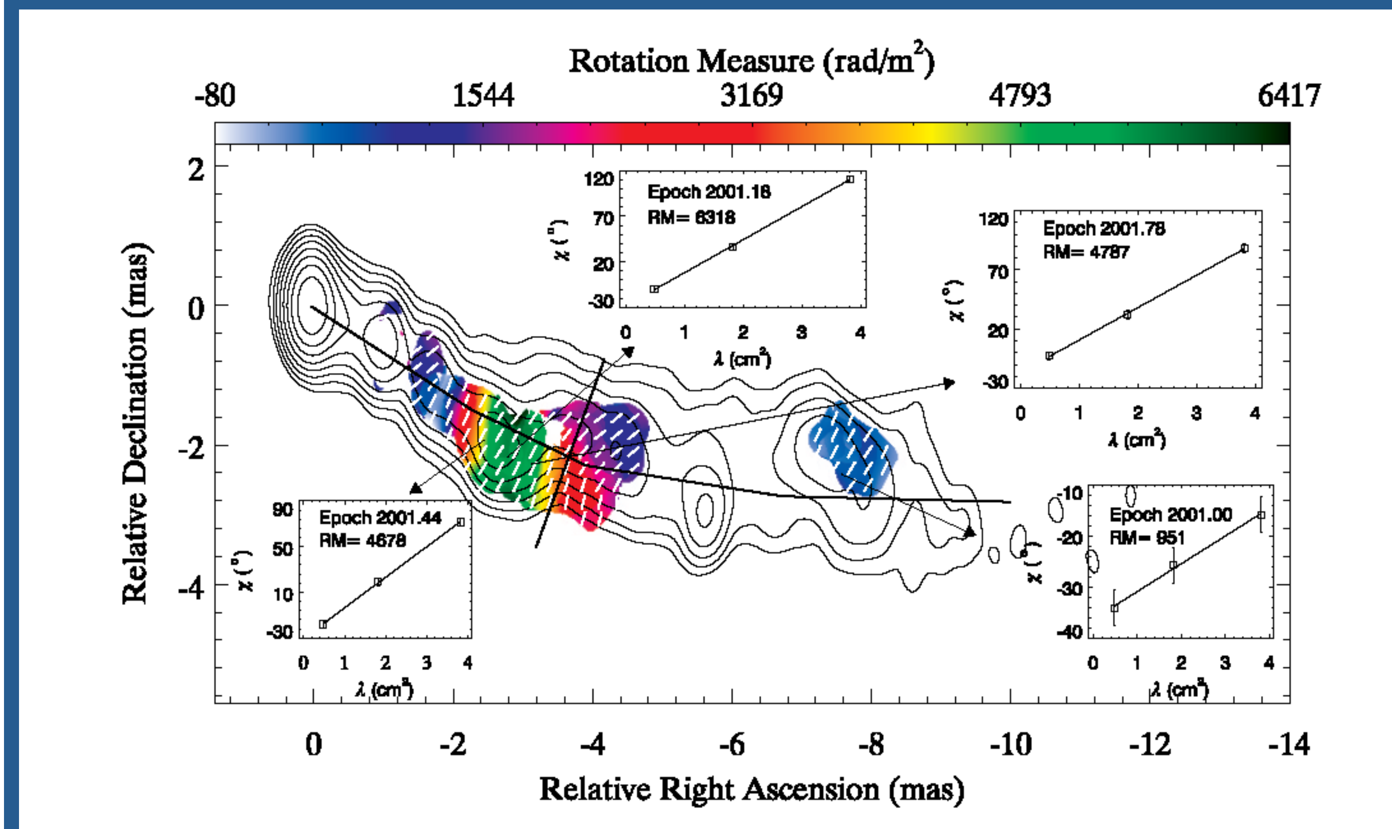

7) Rotation Measures: 3C120 (Gomez et al. 2008)

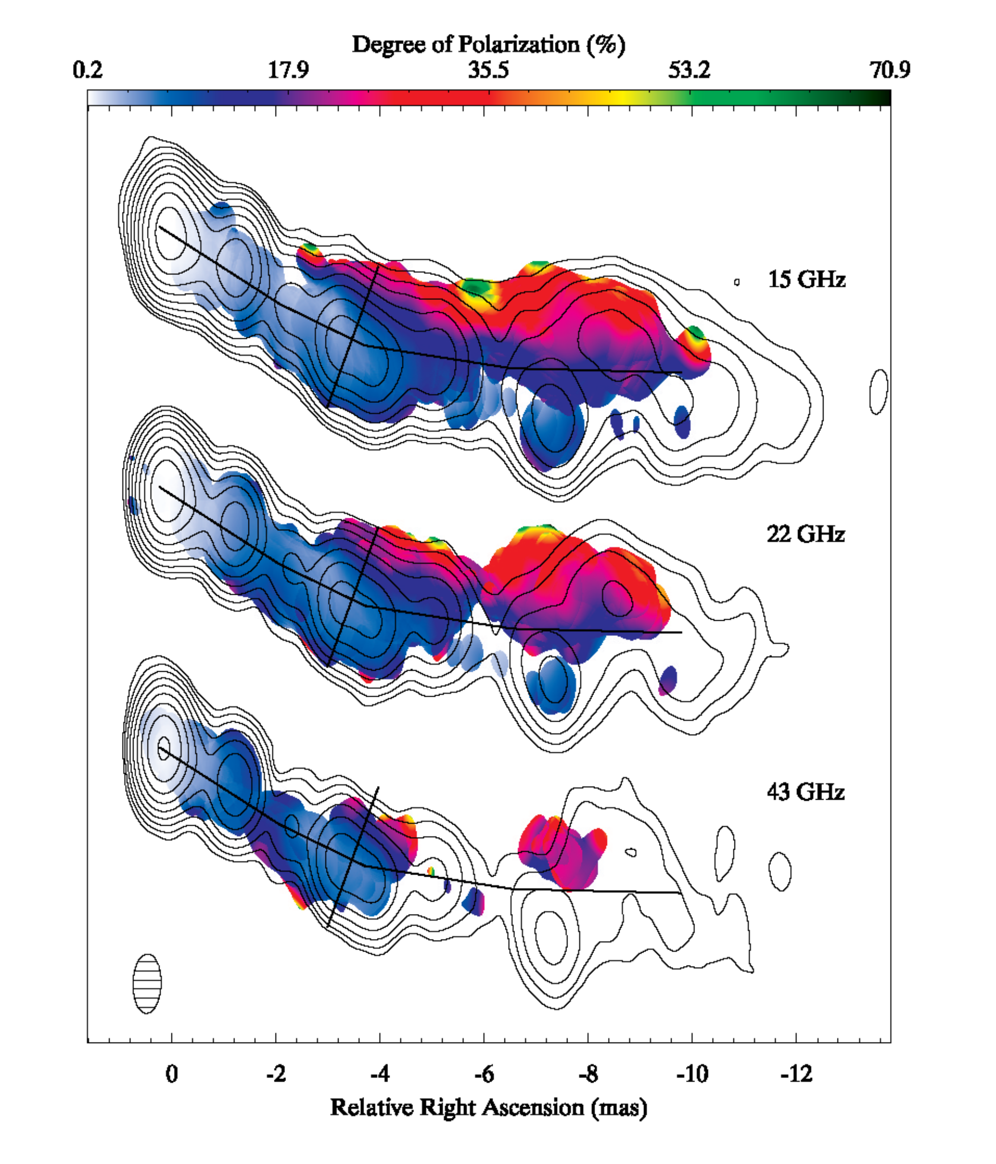

The fractional polarization structure is striated, with high fractional polarization towards the edges of the jet, and low polarization along the center line.

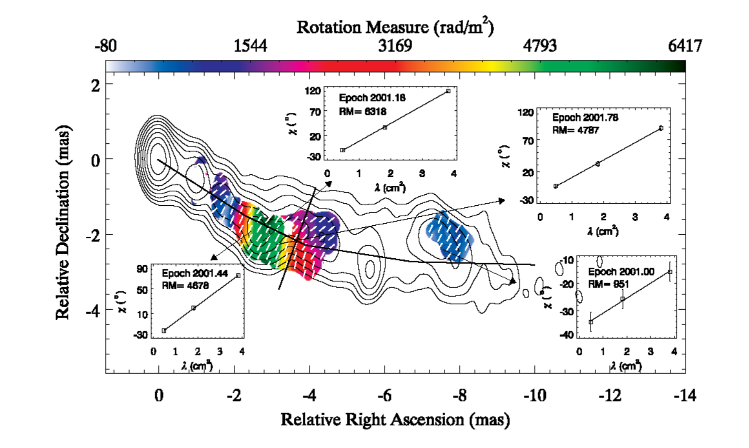

7) Rotation Measure gradients: 3C120 (Gomez et al. 2008)

Upper: transverse slices in fractional polarization at three frequencies.

The black line is Rotation Measure.

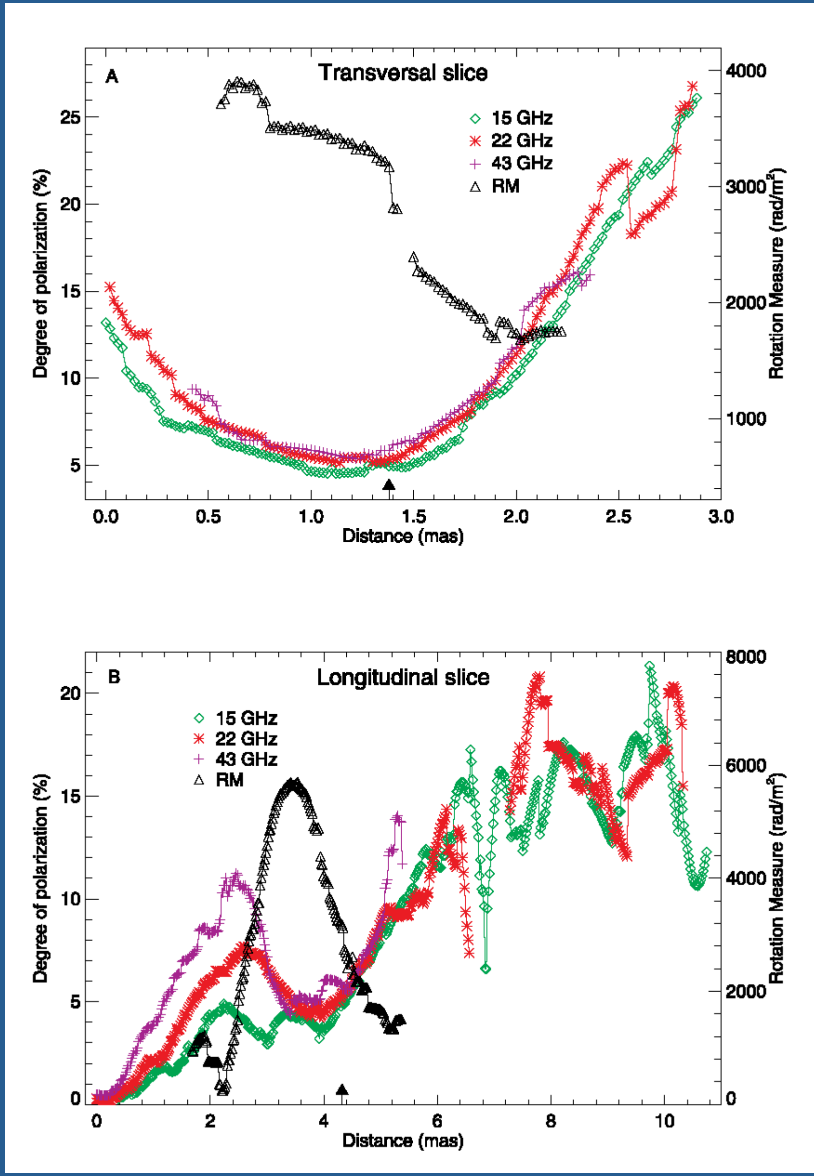

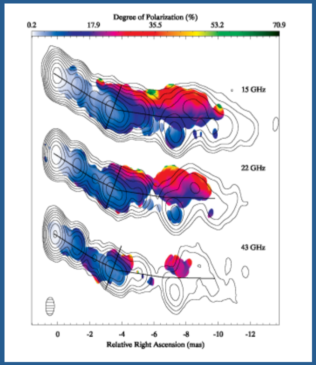

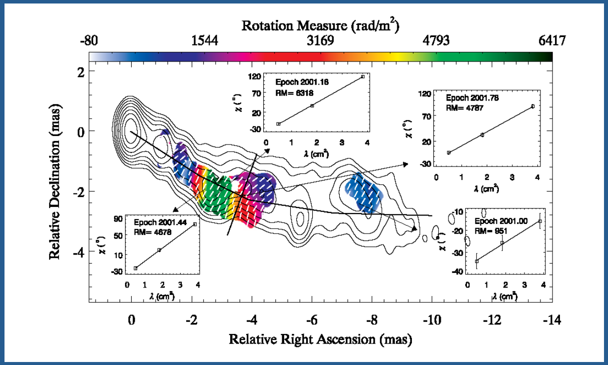

7) Rotation Measure gradients: 3C120 (Gomez et al. 2008)

Upper: transverse slice in fractional polarization at three frequencies.

The black line is Rotation Measure.

Lower: longitudinal slice in fractional polarization at three frequencies.

The Rotation Measure (black line) peaks at a dip in % polarization, and is most likely due to interaction with an external cloud.

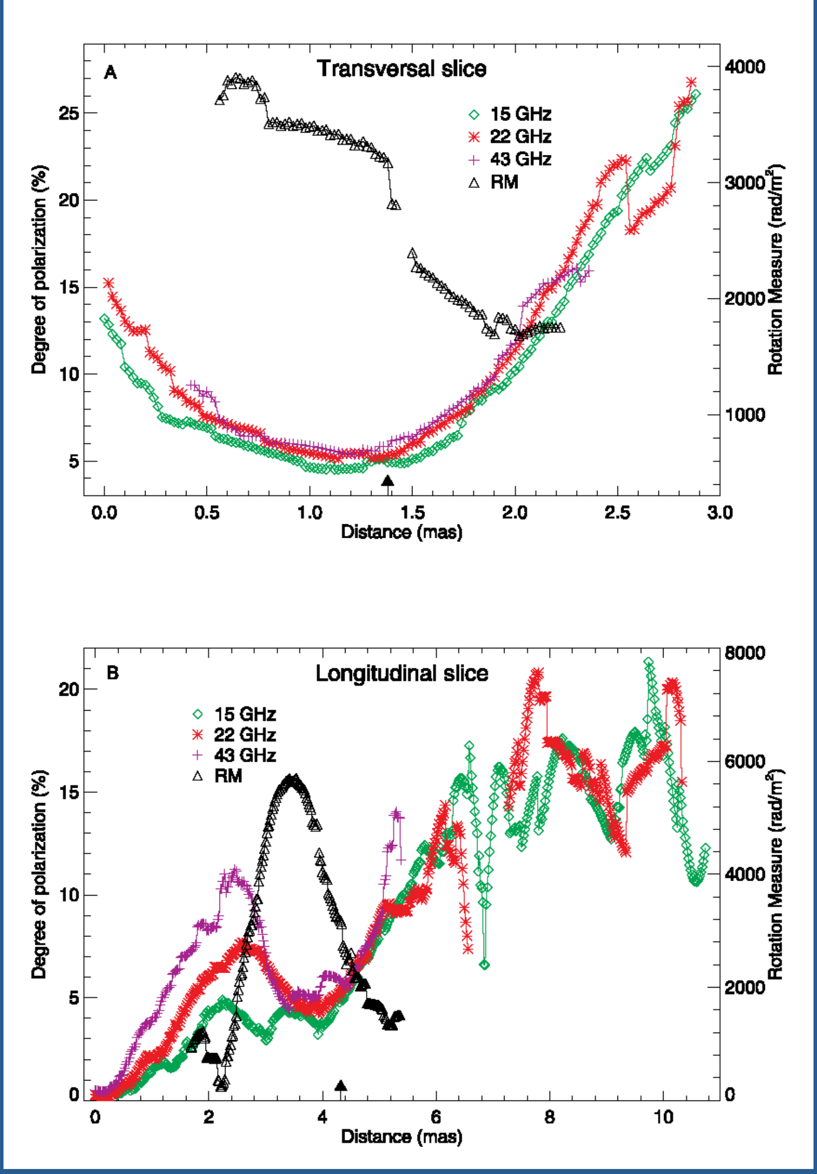

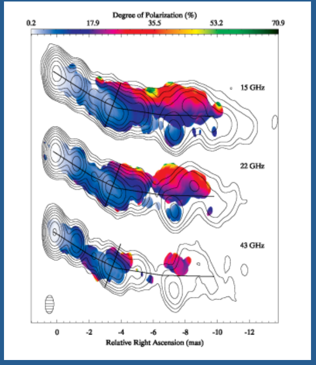

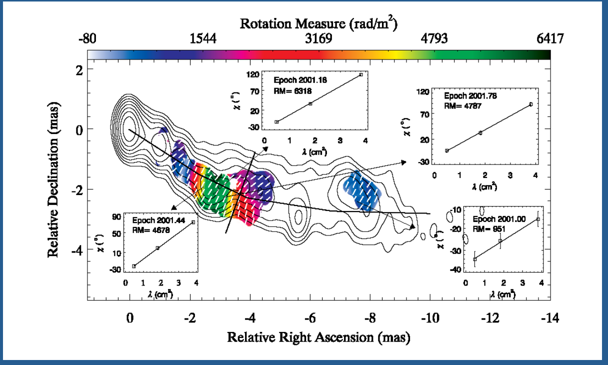

7) Rotation Measure gradients: 3C273 (T. Chen Ph.D. 2005)

6 epochs in 1999 & 2000 at 8, 15 & 22 GHz

Middle: Polarized intensity. Tick marks show the "B field" (EVPA + π/2), corrected for Faraday rotation.

The B field is nearly everywhere aligned with the jet direction.

Lower: Rotation measure. The transverse gradients are clear.

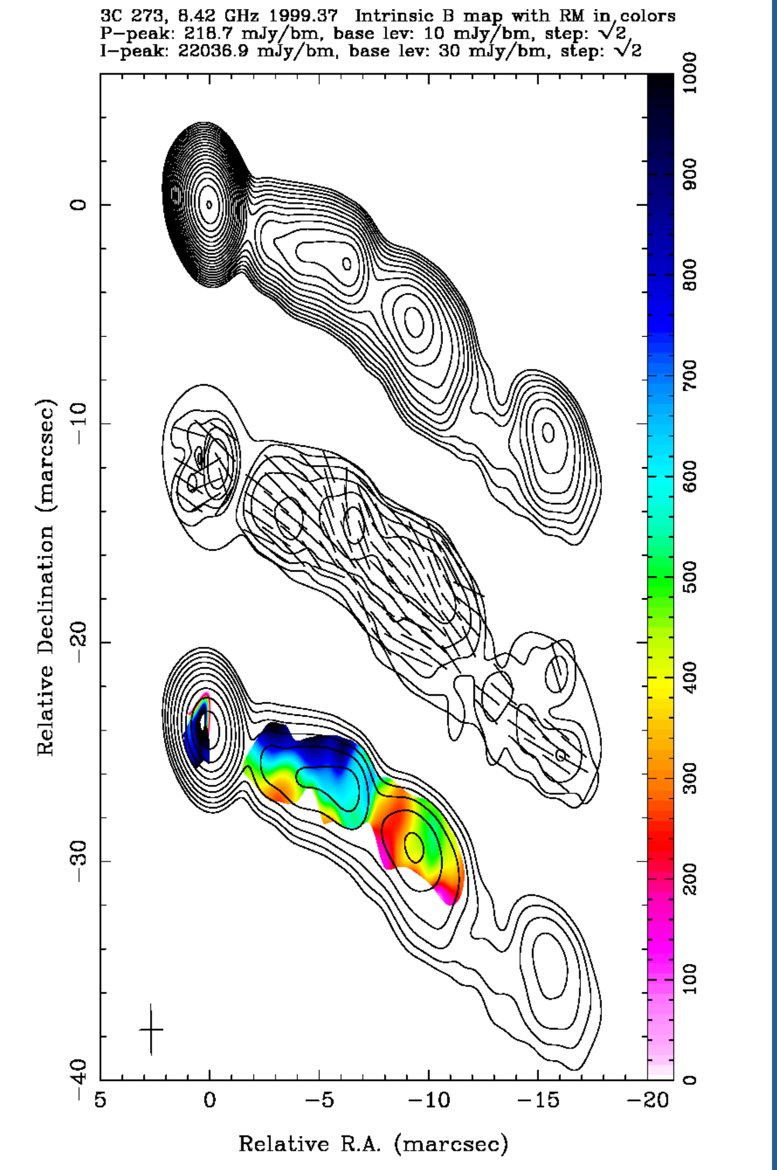

Figure 3.19: (b). Intrinsic B field with RM in colors, 1999.37.

7) Rotation Measure gradients: 3C273 (T. Chen Ph.D. 2005)

Average of 6 polarization images to improve SNR

Top and bottom: plots of EVPA and p versus λ^2 at 6 locations.

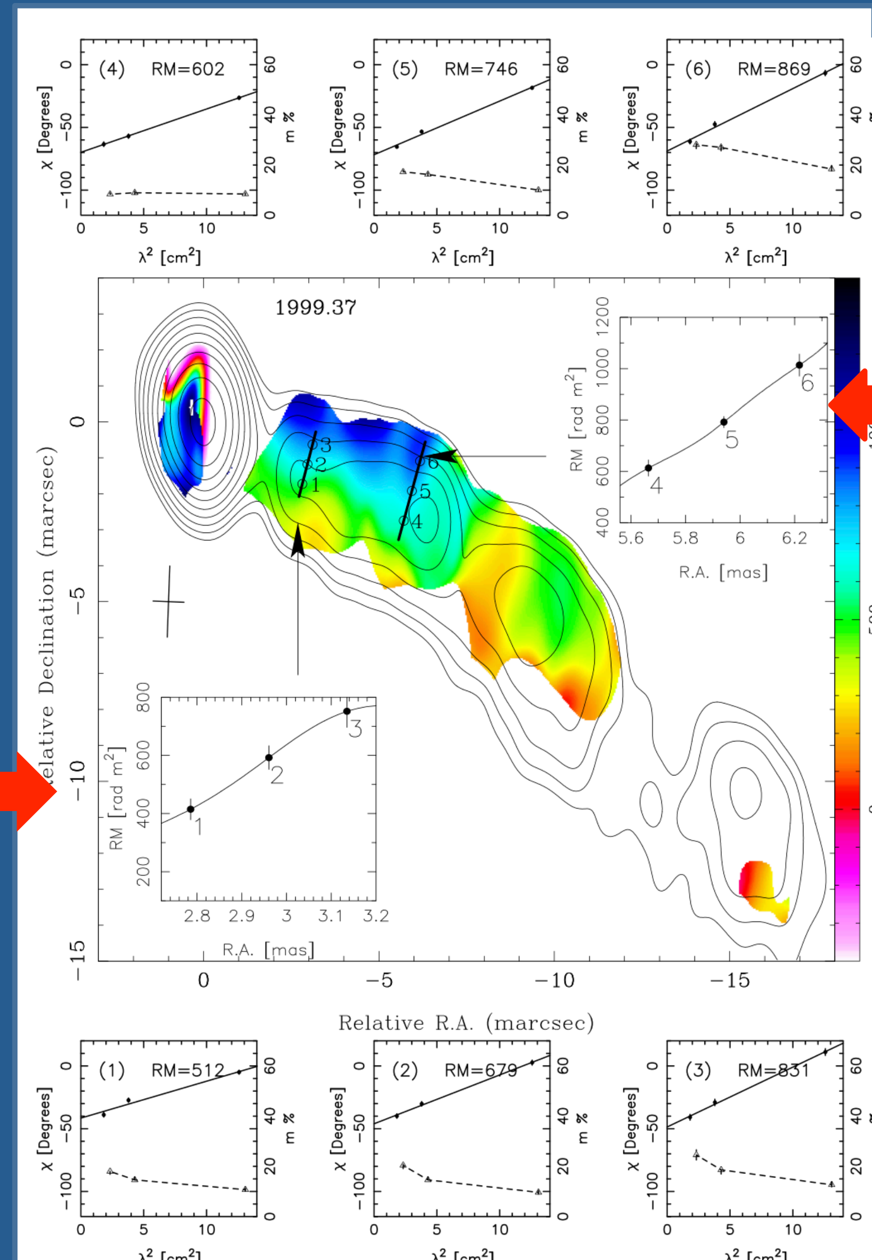

transverse RM slice

transverse RM slice

<u>The transverse gradient in RM can be seen over most of the length of the jet.</u>

7) Rotation Measure gradients: interpretation

A RM gradient suggests a *toroidal* component of the magnetic field (and hence by Ampère's Law, a jet current)

7) Rotation Measure gradients: interpretation

A RM gradient suggests a *toroidal* component of the magnetic field (and hence by Ampère's Law, a jet current)

A *helical* magnetic field requires a poloidal component of comparable magnitude *that is vector ordered*.

7) Rotation Measure gradients: interpretation

A RM gradient suggests a toroidal component of the magnetic field (and hence by Ampère's Law, a jet current)

A *helical* magnetic field requires a poloidal component of comparable magnitude *that is vector ordered*.

Viewed from most directions, a helical field exhibits strong transverse asymmetries in both total intensity and polarization.

Laing, Canvin and Bridle 2006

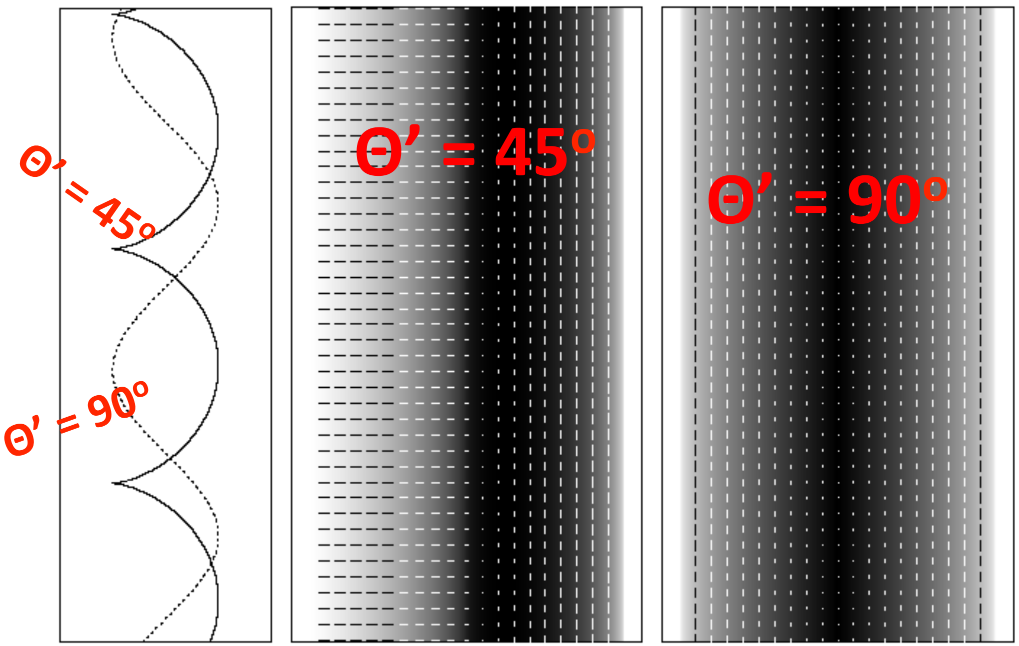

Fig. 3. Total intensity and linear polarization from a (non-relativistic) jet containing a helical magnetic field of pitch angle 45° at angles to the line of sight of $\theta = 45°$ and 90°. Left: sketch showing the projection of field lines on the plane of the sky. Full line, $\theta = 45°$; dotted line, $\theta = 90°$. Middle and right: grey-scales of total intensity with superposed vectors whose lengths are proportional to the degree of polarization and directions along the apparent magnetic field. Middle: $\theta = 45°$; right: $\theta = 90°$.

7) Rotation Measure gradients: a model (J. Mizrahi 2007)

These problems are greatly alleviated if most of the poloidal field is NOT vector ordered. Mizrahi's model contains a uniform current density (which gives the transverse RM gradient) plus sheared loops of field (which give the net magnetic field aligned with the jet.)

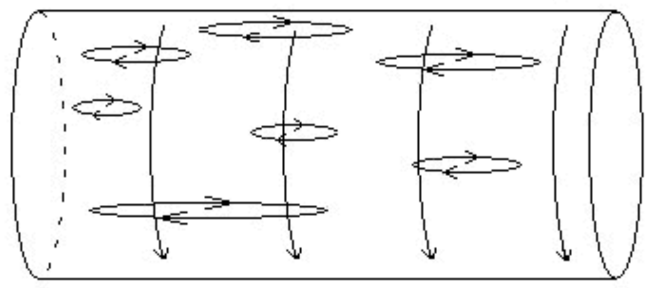

Figure 4: Model of magnetic fields

7) Rotation Measure gradients: a model (J. Mizrahi 2007)

These problems are greatly alleviated if most of the poloidal field is NOT vector ordered. Mizrahi's model contains a uniform current density (which gives the transverse RM gradient) plus sheared loops of field (which give the net magnetic field aligned with the jet.)

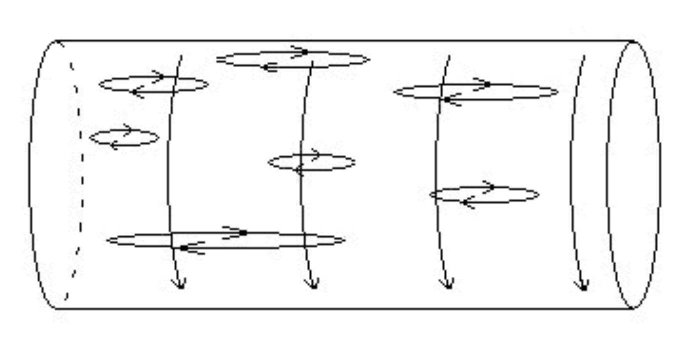

Figure 4: Model of magnetic fields

The resulting polarization can be calculated analytically for α = -1. Model (left) and observed (right) transverse slices of fractional polarization in 3C273.

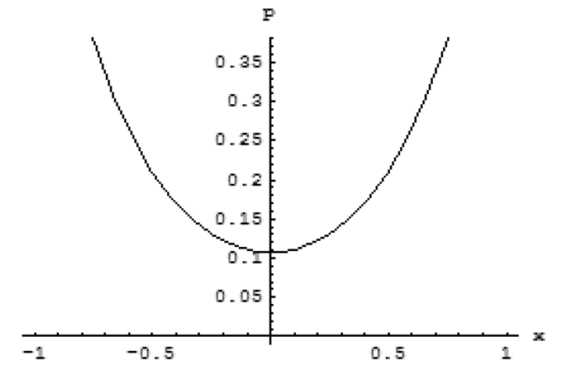

model

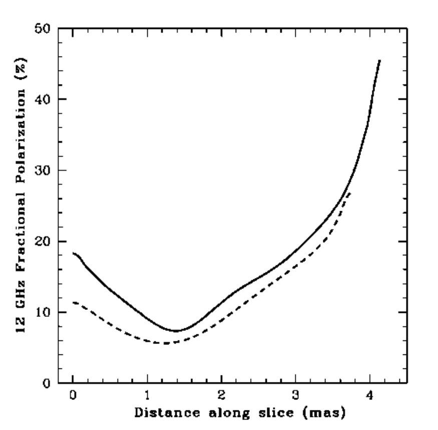

Taylor & Zavala 2005

8) Circular polarization

15 GHz   Homan & Lister 2006

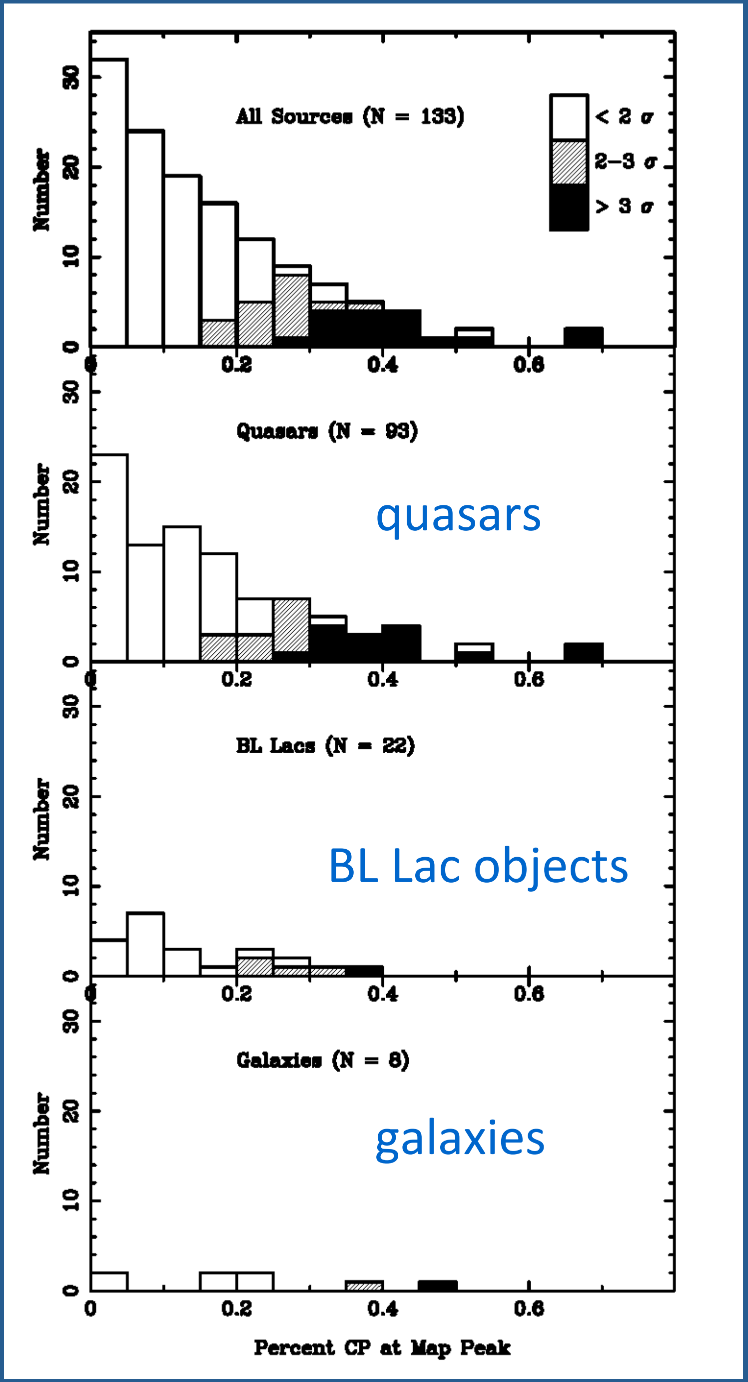

8) Circular polarization

15 GHz   Homan & Lister 2006

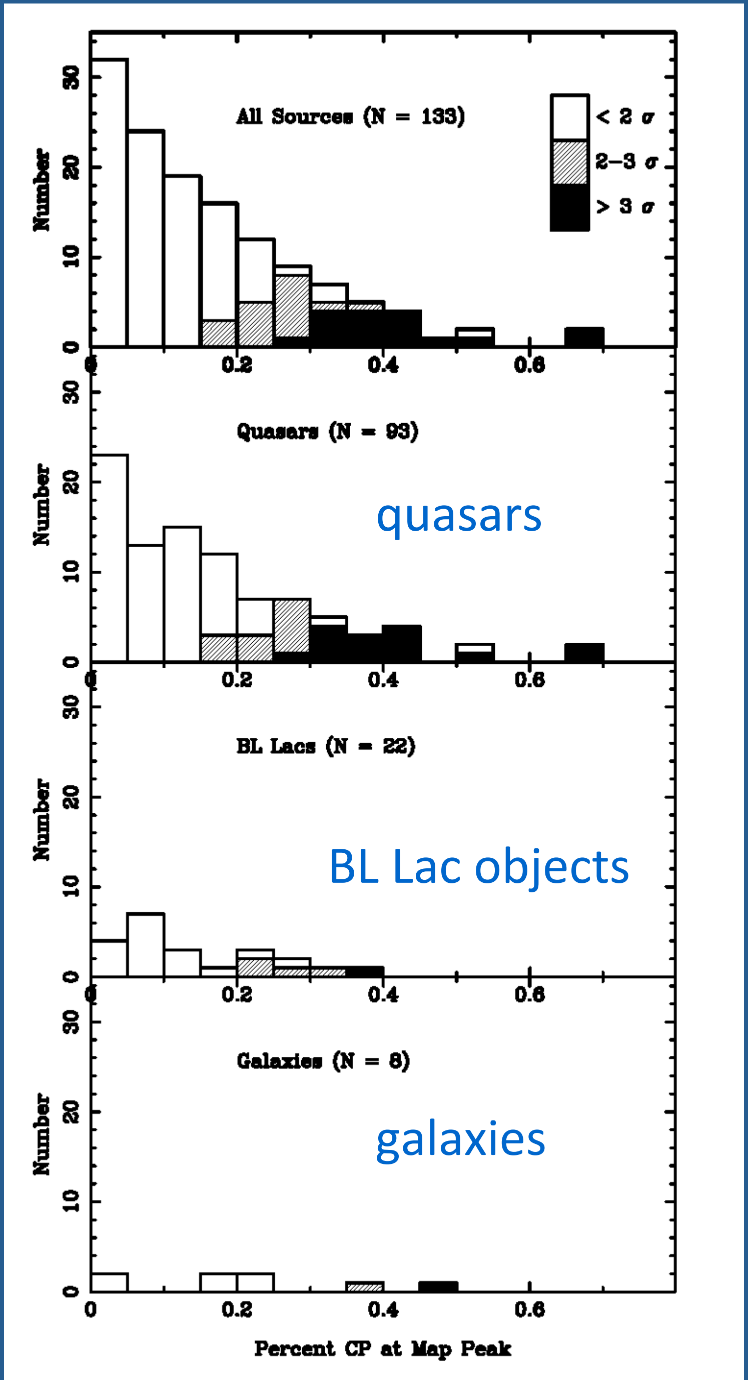

The two main ways of generating circular polarization are

(1) the intrinsic CP of synchrotron radiation ($p_c \sim 1/\gamma_e$)
(2) Faraday conversion of linear to circular. For useful expressions see Wardle & Homan 2003.

8) Circular polarization

15 GHz   Homan & Lister 2006

No obvious correlation between CP and LP (also true at 5 GHz, see Homan et al 2001, and Rayner et al 2000 (ATCA))

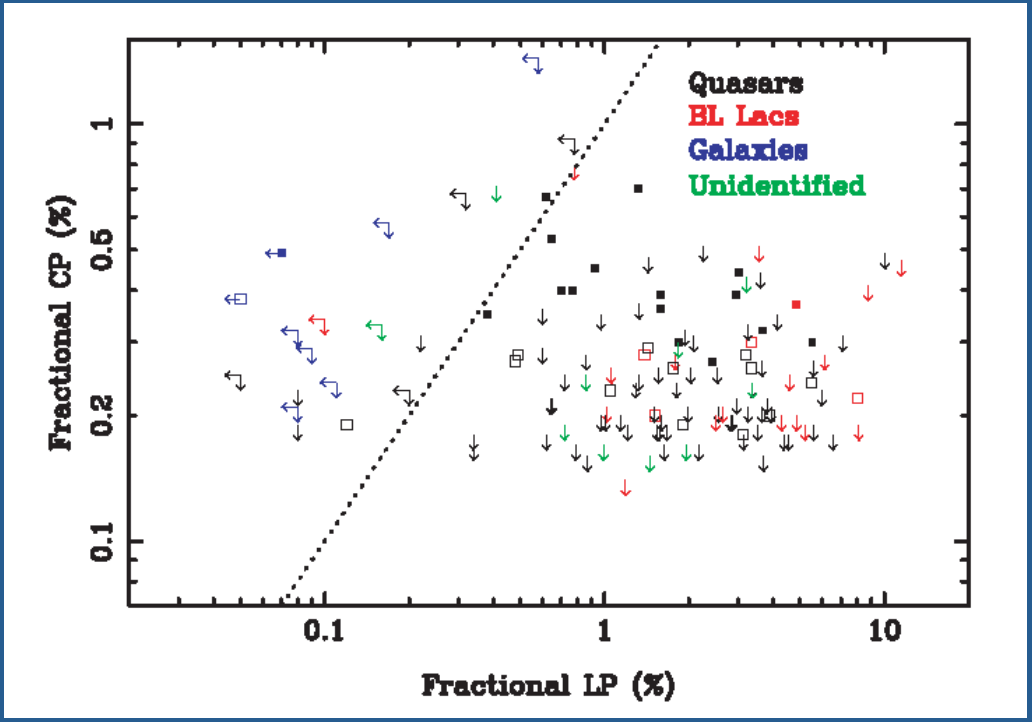

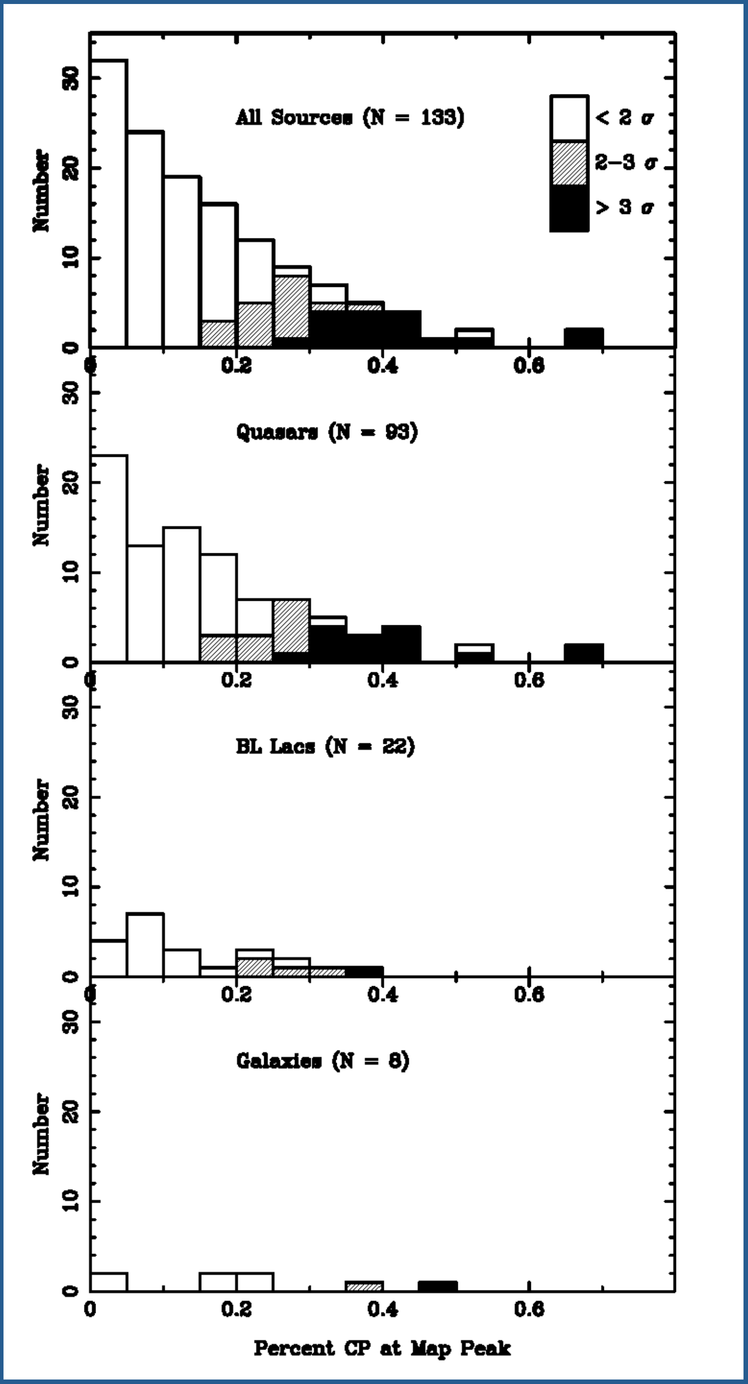

8) Circular polarization

15-22-43 GHz Vitrishchak et al 2008

Table 2. Comparison with MOJAVE CP.

Source	15 GHz Our result m_c (per cent)	15 GHz MOJAVE result m_c (per cent)	Comments
0109+224	-0.24 ± 0.09	<0.25	Our measurement consistent with upper limit
0133+476	-0.32 ± 0.09	-0.18 ± 0.09	
0300+470	-0.30 ± 0.10	<0.21	
0823+033	$+0.20 \pm 0.09$	<0.26	Our measurement consistent with upper limit
0851+202	-0.15 ± 0.08	-0.20 ± 0.08	
	-0.19 ± 0.08		
1055+018	$+0.52 \pm 0.10$	$+0.32 \pm 0.09$	
1156+295	-0.28 ± 0.11	-0.27 ± 0.09	
1253−055	$+0.19 \pm 0.11$	$+0.30 \pm 0.08$	
	$+0.83 \pm 0.10$		
	$+0.26 \pm 0.09$		
1334−127	$+0.28 \pm 0.09$	$+0.29 \pm 0.10$	
1510−089	<0.22	$+0.20 \pm 0.09$	We find $+0.49 \pm 0.19$ at 22 GHz
1633+382	-0.34 ± 0.06	-0.39 ± 0.09	
1749+096	-0.19 ± 0.08	<0.14	
	-0.21 ± 0.08		
2145+067	-0.45 ± 0.09	<0.26	
2223−052	-0.20 ± 0.07	<0.22	Our measurement consistent with upper limit
2230+114	-0.61 ± 0.08	<0.19	
2251+158	$+0.17 \pm 0.10$	$+0.23 \pm 0.10$	

8) Circular polarization

15-22-43 GHz Vitrishchak et al 2008

Fractional CP is <u>higher</u> at 43 GHz. . . .

. . . This is probably the signature of an inhomogeneous Blandford-Königl type core, where we expect the CP spectrum to rise with frequency for both intrinsic and Faraday conversion mechanisms (Wardle & Homan 2003).

This image of PKS 1055+018 suggests intrinsic CP in a toroidal field.

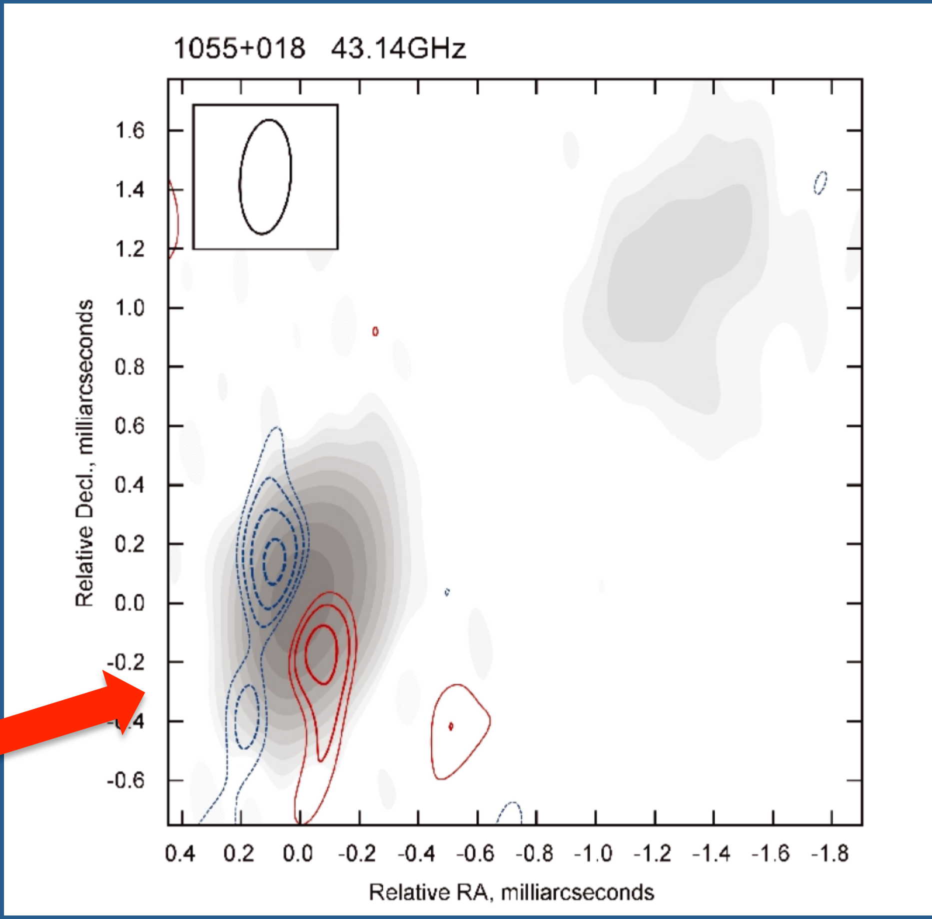

8) Circular polarization: variability

Long-term Frequency-dependent Differences in Polarity

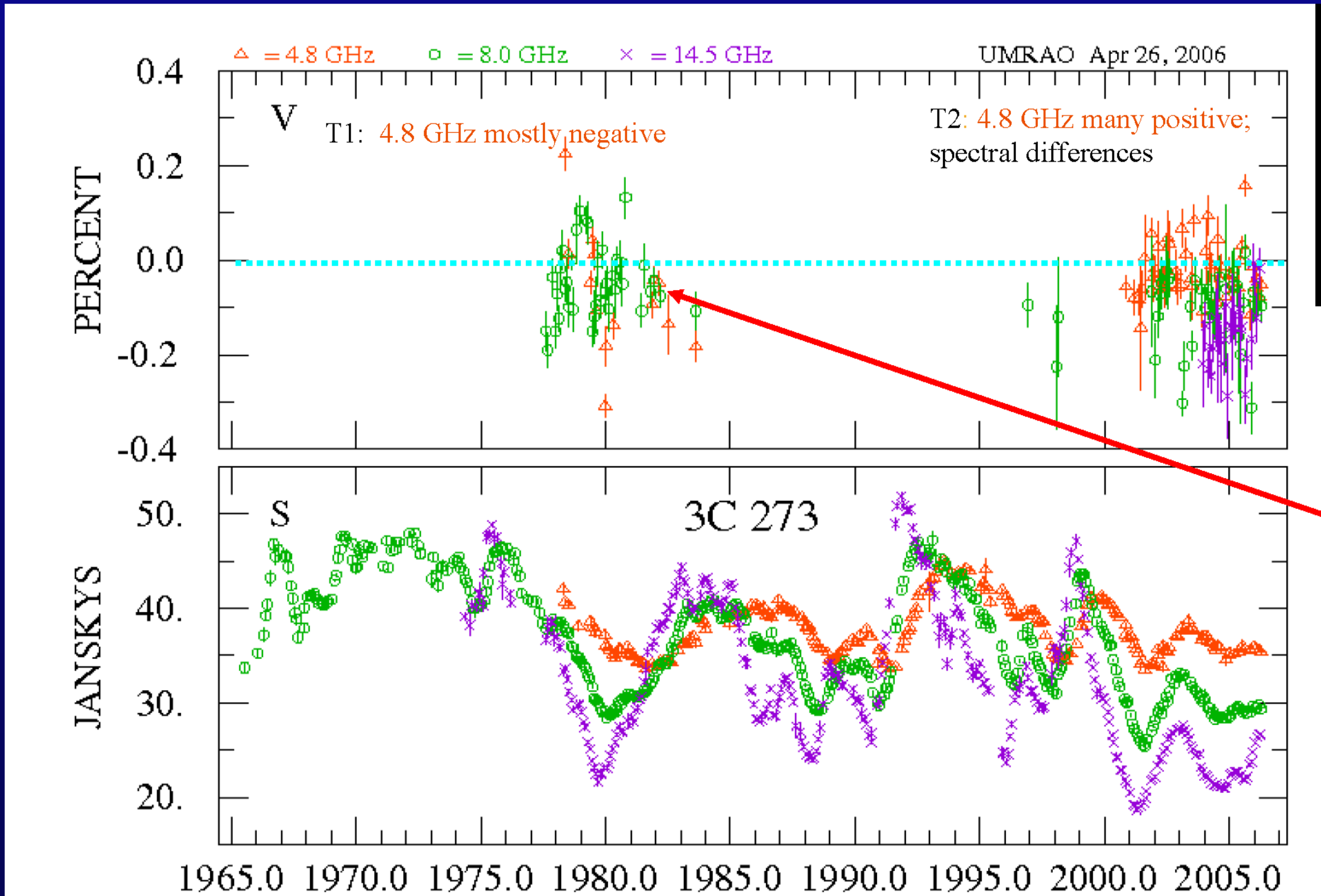

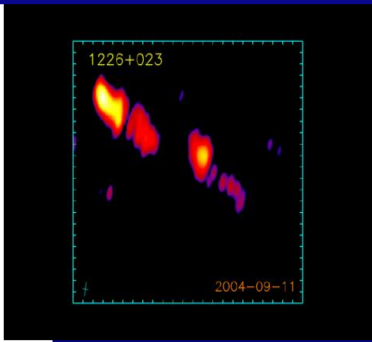

MOJAVE I image

Aller 2006

Parkes 5 GHz:
1977-82 negative

8) Circular polarization: “Full Polarization Spectra”

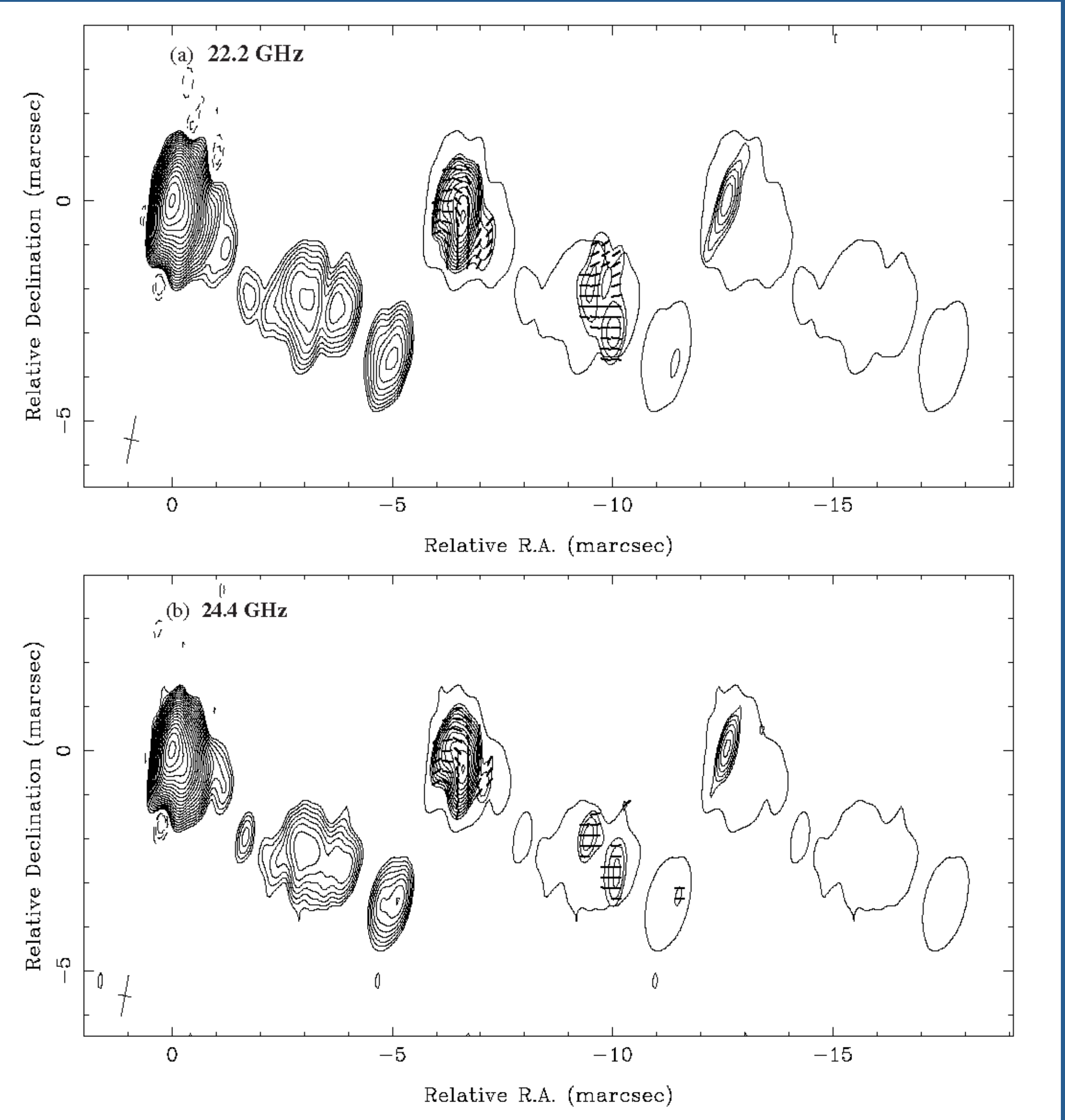

18 AGN observed with the VLBA at 8.0, 8.8, 12.4, 15.4, 22.2 & 22.4 GHz + detailed modeling of *the spectra* of all 4 Stokes parameters.

3C 279: Homan et al. 2009

8) Circular polarization: "Full Polarization Spectra"

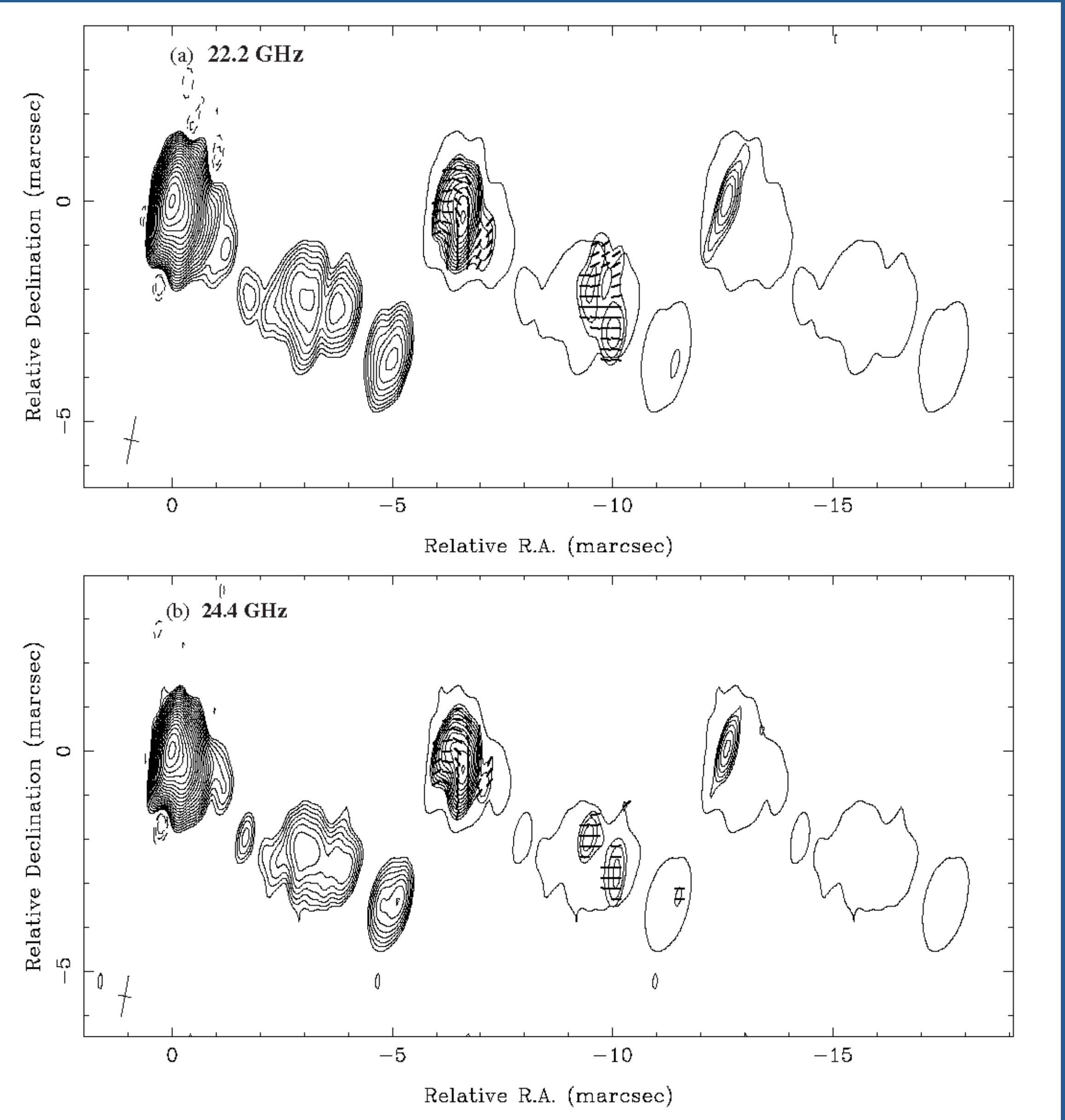

18 AGN observed with the VLBA at 8.0, 8.8, 12.4, 15.4, 22.2 & 22.4 GHz + detailed modeling.

3C 279: Homan et al. 2009

Estimate:

1. Vector ordering of the magnetic field;
2. magnetic flux (=magnetic flux at the black hole?);
3. positron fraction;
4. low-energy cutoff in the electron energy spectrum.

9) The Event Horizon Telescope

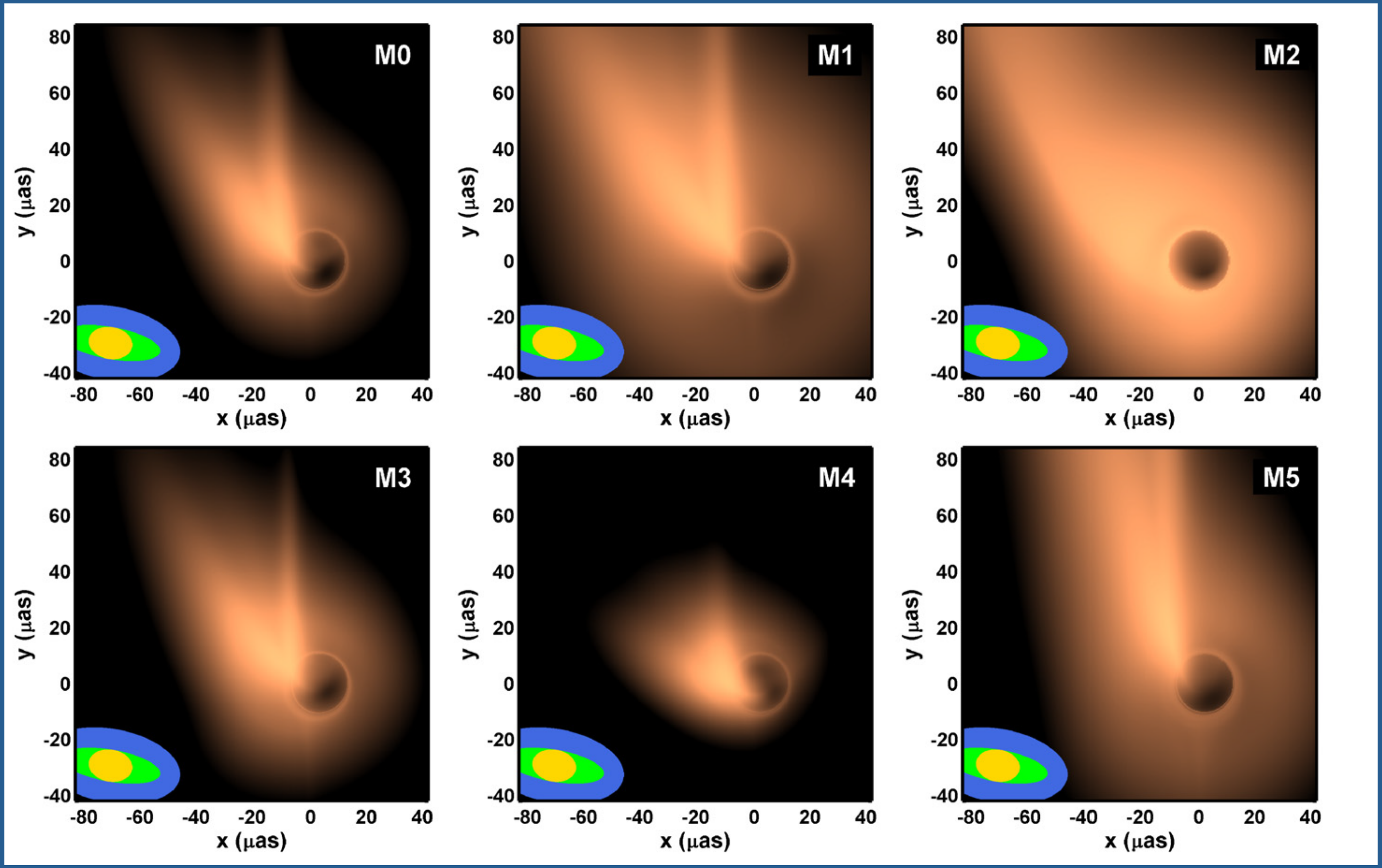

The theoreticians are having so much fun!

M87: Broderick & Loeb 2009

9) The Event Horizon Telescope

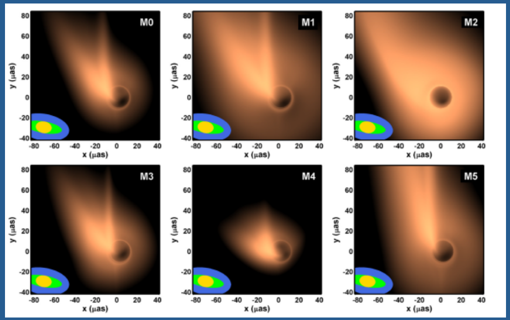

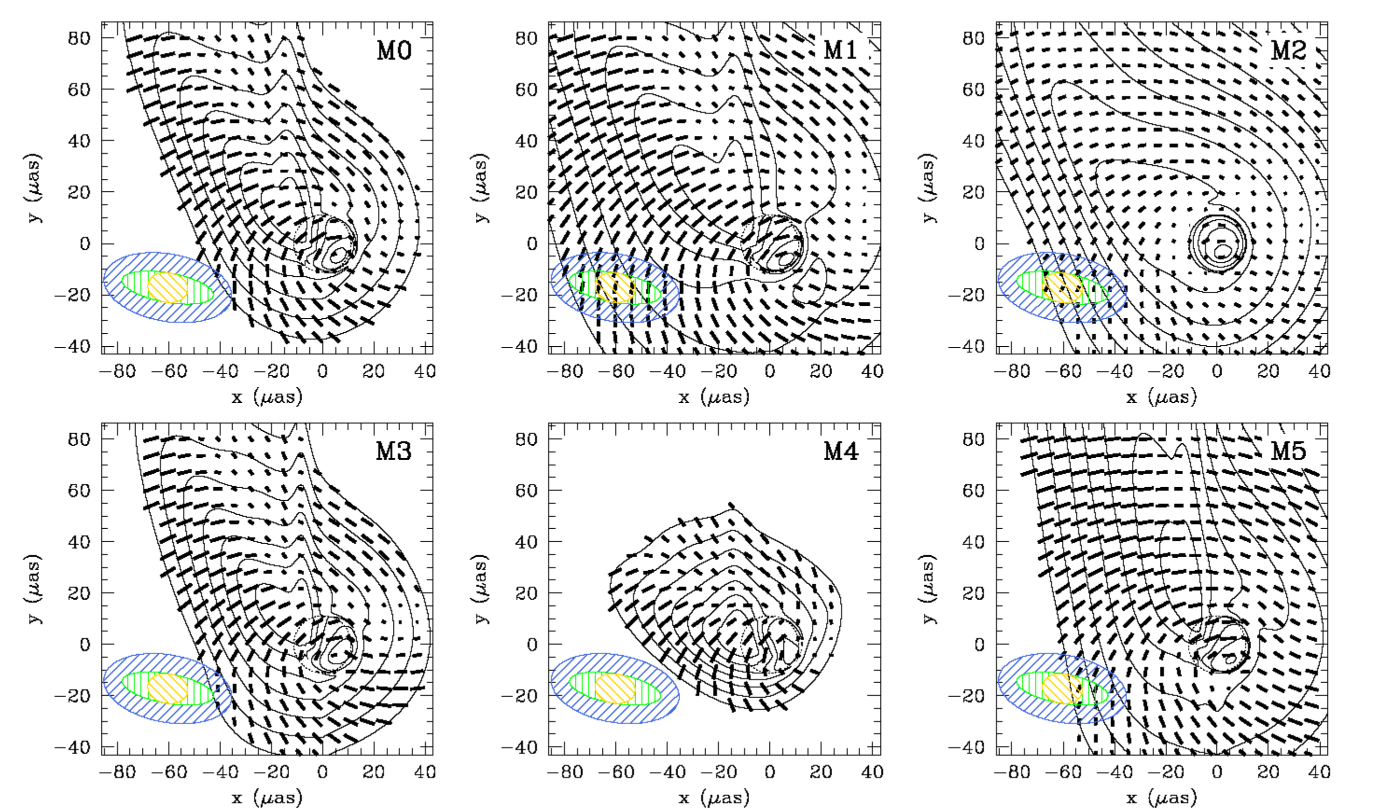

M87: Broderick & Loeb 2009

9) The Event Horizon Telescope

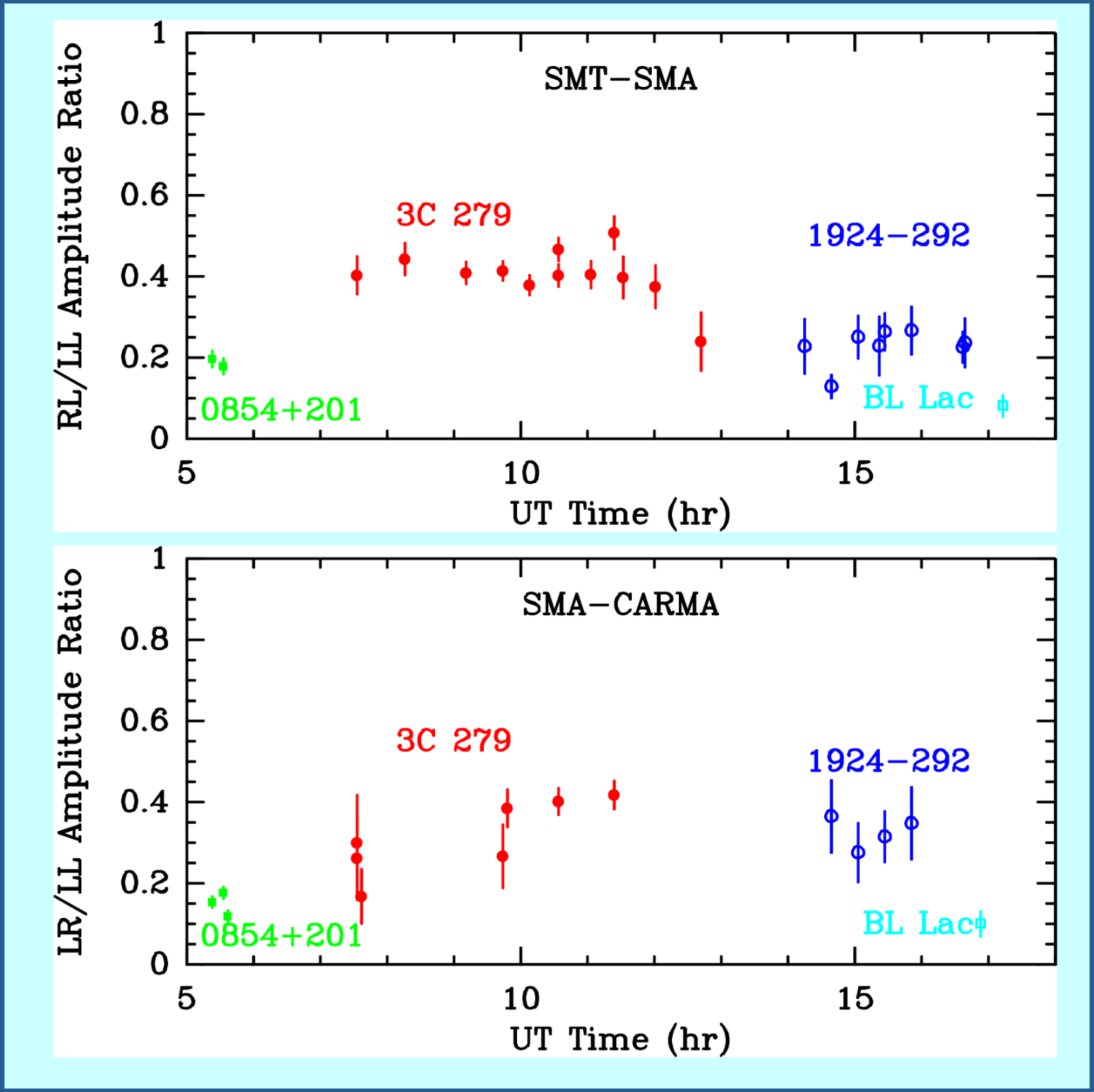

Polarized fringes at 230 GHz (λ 1.3 mm) between Hawaii and Arizona, and Hawaii and California.

Fish et al 2013; poster at AAS meeting

9) The Event Horizon Telescope

ALMA makes this very feasible. Stay tuned.

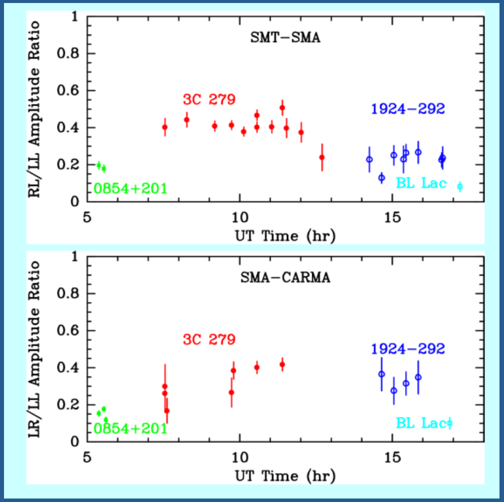

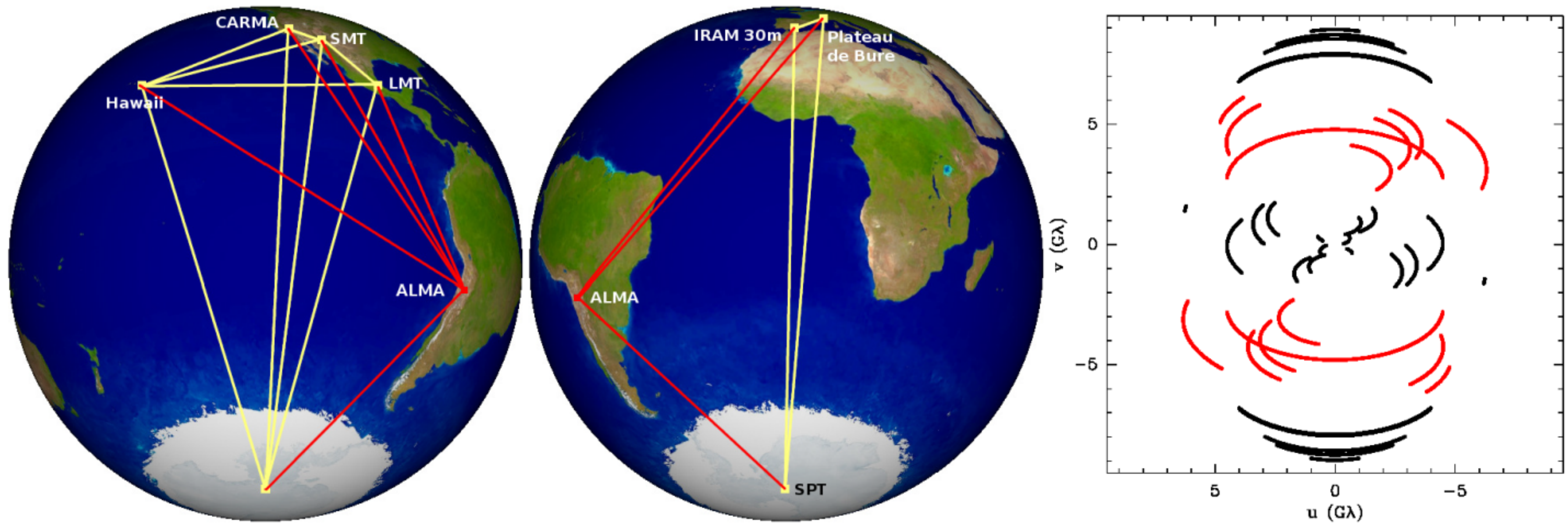

FIG. 2.— Left and middle: The potential 1.3 mm VLBI network as viewed from the declination of Sgr A*. Right: The corresponding (u, v) coverage. Baselines to ALMA are marked in red in all panels.